NAVAL POSTGRADUATE SCHOOL
Monterey, California

THESIS

COHERENT/NONCOHERENT DETECTION OF
COHERENT OPTICAL HETERODYNE
DPSK-CDMA AND MFSK-CDMA SIGNALS

by

David Andrew Jakubek

December 1991

Thesis Advisor: R. Clark Robertson
Co-Advisor: Tri T. Ha

Approved for public release; distribution is unlimited

UNCLASSIFIED
SECURITY CLASSIFICATION OF THIS PAGE

REPORT DOCUMENTATION PAGE

Form Approved
OMB No 0704-0188

1a REPORT SECURITY CLASSIFICATION UNCLASSIFIED	1b RESTRICTIVE MARKINGS
2a SECURITY CLASSIFICATION AUTHORITY	3 DISTRIBUTION / AVAILABILITY OF REPORT Approved for public release; distribution is unlimited
2b DECLASSIFICATION / DOWNGRADING SCHEDULE	
4 PERFORMING ORGANIZATION REPORT NUMBER(S)	5 MONITORING ORGANIZATION REPORT NUMBER(S)
6a NAME OF PERFORMING ORGANIZATION Naval Postgraduate School 6b OFFICE SYMBOL (If applicable) EC	7a NAME OF MONITORING ORGANIZATION Naval Postgraduate School
6c ADDRESS (City, State, and ZIP Code) Monterey, CA 93943-5000	7b ADDRESS (City, State, and ZIP Code) Monterey, CA 93943-5000
8a NAME OF FUNDING / SPONSORING ORGANIZATION 8b OFFICE SYMBOL (If applicable)	9 PROCUREMENT INSTRUMENT IDENTIFICATION NUMBER
8c ADDRESS (City, State, and ZIP Code)	10 SOURCE OF FUNDING NUMBERS PROGRAM ELEMENT NO / PROJECT NO / TASK NO / WORK UNIT ACCESSION NO

11 TITLE (Include Security Classification)
COHERENT/NONCOHERENT DETECTION OF COHERENT OPTICAL HETERODYNE DPSK-CDMA AND MFSK-CDMA SIGNALS

12 PERSONAL AUTHOR(S)
JAKUBEK, David A.

13a TYPE OF REPORT	13b TIME COVERED	14 DATE OF REPORT (Year, Month, Day)	15 PAGE COUNT
Engineer's Thesis	FROM _____ TO _____	1991 December	103

16 SUPPLEMENTARY NOTATION The views expressed in this thesis are those of the author and do not reflect the official policy or position of the Department of Defense or US Government.

17 COSATI CODES			18 SUBJECT TERMS (Continue on reverse if necessary and identify by block number)
FIELD	GROUP	SUB-GROUP	coherent optical communications; optical heterodyne communications; spread spectrum; CDMA; MFSK modulation; DPSK modulation

19 ABSTRACT (Continue on reverse if necessary and identify by block number)

The system performance of a coherent optical heterodyne communication system is analyzed for MFSK-CDMA and DPSK-CDMA signalling. The analysis determines the effect that receiver thermal noise, photodetector shot noise, laser phase noise, and multiple user noise has on the system performance.

For the single user system performance, the probability of bit error of the system as a function of E_b/N_o is calcuated for laser linewidth-to-bit rate ratios from 0.1 to 0.01. For both MFSK and DPSK, the system performance is most affected by laser phase noise at higher linewidth-to-bit rate ratios.

The multiple user analysis for MFSK-CDMA and DPSK-CDMA is determined by calculating the probability of bit error as a function of the number

20 DISTRIBUTION / AVAILABILITY OF ABSTRACT	21 ABSTRACT SECURITY CLASSIFICATION
☒ UNCLASSIFIED/UNLIMITED ☐ SAME AS RPT ☐ DTIC USERS	UNCLASSIFIED
22a NAME OF RESPONSIBLE INDIVIDUAL ROBERTSON, R.C.	22b TELEPHONE (Include Area Code) 408-646-2383 22c OFFICE SYMBOL EC/Rc

DD Form 1473, JUN 86 *Previous editions are obsolete*

S/N 0102-LF-014-6603

SECURITY CLASSIFICATION OF THIS PAGE
UNCLASSIFIED

19. cont.

of users for various laser linewidth-to-bit rate ratios and codelengths. The observations made for the single user case concerning the effects of laser phase noise are also observed for the multiple user case. When the effects of the laser phase noise no longer dominate system performance then MFSK-CDMA and DPSK-CDMA can be used to increase the user capacity of optical fiber systems.

Approved for public release; distribution is unlimited.

Coherent/Noncoherent Detection of Coherent Optical Heterodyne DPSK-CDMA and MFSK-CDMA Signals

by

David A. Jakubek
Lieutenant, United States Navy
B.S., University of Pittsburgh, 1984

Submitted in partial fulfillment
of the requirements for the degrees of

MASTER OF SCIENCE IN ELECTRICAL ENGINEERING

and

ELECTRICAL ENGINEER

from the

NAVAL POSTGRADUATE SCHOOL
December 1991

ABSTRACT

The system performance of a coherent optical heterodyne communication system is analyzed for MFSK-CDMA and DPSK-CDMA signalling. The analysis determines the effect that receiver thermal noise, photodetector shot noise, laser phase noise, and multiple user noise has on the system performance.

For the single user system performance, the probability of bit error of the system is calculated as a function of E_b/N_0 for laser linewidth-to-bit rate ratios from 0.1 to 0.01. For both MFSK and DPSK, the system performance is most affected by laser phase noise at higher linewidth-to-bit rate ratios.

The multiple user analysis for MFSK-CDMA and DPSK-CDMA is determined by calculating the probability of bit error as a function of the number of users for various laser linewidth-to-bit rate ratios and codelengths. The observations made for the single user case concerning the effects of laser phase noise are also observed for the multiple user case. When the effects of the laser phase noise no longer dominate system performance, then MFSK-CDMA and DPSK-CDMA can be used to increase the user capacity of optical fiber systems.

TABLE OF CONTENTS

I. INTRODUCTION

Optical fiber communications is undergoing an evolution that is similar to that which occurred for conventional wire and wireless communications. From the spark-gap transmissions that were first sent over wire and then free space to the spread spectrum techniques currently researched today, the history of baseband and radio frequency communications provides a direction for the development of improved optical fiber communication systems. This is now possible due to the advances in the research and development of coherent optical fiber communication systems. A brief description of coherent optical fiber communication systems will be developed followed by a description of future optical fiber communication systems proposed in this thesis.

Like the spark-gap transmissions of Morse Code over wire and then free space, optical fiber communications originated as an incoherent communication method in order to transfer information, that is intensity modulation followed by direct detection. For optical communications, incoherent communication implies that a coherent carrier, that is, a stable frequency oscillator, is not required for transmission. A wideband light source such as an incandescent light or light emitting diode can be used. Therefore, no information is present in the frequency or phase of the signal. Only the

amplitude of the signal is varied in order to transmit information. Intensity modulation implies that the light intensity is modulated linearly with respect to the input signal voltage. To date, intensity modulation has been the standard modulation technique in optical fiber communications. Detection of these signals is not sophisticated since no frequency conversion or any other signal processing is involved. Direct detection is used to receive this signal. Direct detection implies that the signal is detected at the optical stage of the receiver. For direct detection of intensity modulated signals, information is obtained by detecting the presence or absence of a transmission by receiving optical energy above or below some threshold level. This is analogous to on-off keying (OOK) baseband signalling used in digital communication systems.

In contrast to incoherent optical communication methods, coherent optical communications techniques depend on a stable oscillating frequency carrier for transmission which is then modulated by an information signal. For these techniques the information is transmitted in the frequency or phase of the signal. Bandpass signalling such as amplitude-shift keying (ASK), frequency-shift keying (FSK), and phase-shift keying (PSK) are examples of coherent communication methods.

Three types of detection methods exist for coherent optical communications: direct detection, heterodyne detection, and homodyne detection. One can easily confuse

coherent optical communications and coherent signalling. Coherent optical communication exists when the information of the signal is modulated on a stable frequency carrier thus allowing either homodyne or heterodyne detection. This requires the linewidth of the transmission source to be relatively narrow. The linewidth of the transmission source is the possible range of frequencies over which the source will vary. An electronic receiver example is a microwave oscillator which typically has a linewidth on the order of magnitude of 1 Hz [Ref. 1:p. 2156]. For optical communications, the best linewidth that has been achieved to date for semiconductor lasers is on the order of magnitude of 10 kHz [Ref. 2:p. 9]. On the other hand, coherent signalling implies that information is present in the signal phase. For coherent signalling both the frequency and phase of the incoming signal are matched at the receiver by a reference signal in order to detect that signal.

For direct detection, the detector converts the modulated optical signal to a baseband signal which contains the information frequencies. Direct detection is considered a coherent optical communication detection method if a stable oscillator is used as the carrier. As stated above direct detection is used to detect the presence or absence of an optical signal above some threshold value to yield a binary result. Direct detection is also used to yield an output that contains frequency information resulting in an analog signal.

In either case, the direct detection method is a relatively easy and cheap method of optical detection since no frequency conversion or signal processing is required.

Heterodyne detection involves the optical combining of the signal beam with a local oscillator beam before detection. The local oscillator beam is at a different frequency than the signal beam, but the two beams must have a high degree of monochromaticity and the same polarization. The two beams form an interference pattern at the detector. The output of the detector is modulated at the difference frequency of the two beams. This is also known as the intermediate frequency (IF). Currently, for coherent optical communications, the IF is chosen to be at radio frequencies (RF) so that conventional RF demodulation methods can be performed on the signals electronically. Heterodyne communications offers improved sensitivity at the cost of a more sophisticated and more difficult method of detection.

Homodyne detection is a special case of heterodyne detection. For homodyne detection, the frequency and phase of the local oscillator are controlled so that they match that of the incoming signal beam. This corresponds to coherent detection previously discussed. Even though this method theoretically provides the best performance of the three detection methods for coherent optical communications, it is also the most difficult to implement.

Over approximately the past ten years, coherent optical fiber communication has been heavily studied and documented. During the early development of optical fiber communications, much of the improvements were due to advances in optical sources and fiber technology. The reception of optical signals was not significantly affected. With improvements in narrowing the linewidth of optical sources, the practical realization of coherent optical fiber receivers became possible.

The benefits of coherent optical communication systems are improved receiver sensitivity and improved frequency selectivity. These benefits can only be achieved by using more sophisticated transmitters and receivers. Here, receiver sensitivity refers to the minimum amount of received signal power which is required to produce a prescribed bit error rate [Ref. 3:p. 16]. The improved receiver sensitivities for optical communication systems allows increased repeater spacing in preexisting optical fiber systems. Increased frequency selectivity allows more channel capacity and better utilization of the enormous bandwidth available on optical fibers. The increased frequency selectivity is exploited in this thesis for the development of the coherent optical heterodyne multiple access communication system.

This thesis concentrates on the detection of coherent optical heterodyne signalling. As stated above, one of the benefits of coherent optical heterodyne communications is

improved sensitivity of the receiver. The heterodyne detection method with its strong local oscillator drastically reduces the effect of thermal noise and shot noise in the receiver, therefore requiring less signal power in order to accurately detect an incoming signal. Unfortunately, the effect of laser phase noise is now a factor. Laser phase noise is an inherent part of semiconductor lasers and is due to sudden phase shifts which occur due to spontaneous emission events within the laser. This causes a broadening of the laser linewidth and is referred to as laser phase noise. For heterodyne communication systems, both the transmit and the local oscillator lasers contribute to the laser phase noise. The effect of laser phase noise is minimized by increasing the symbol rate. In this work, the performance of both multiple frequency-shift keying (MFSK) and differential phase-shift keying (DPSK) receivers in the presence of receiver thermal noise, photodetector shot noise, and laser phase noise will be examined for coherent optically heterodyned communication systems.

Another problem that is addressed in this thesis is how to provide access to the system for increasing number of users without having a dedicated channel for each user. Currently, wavelength division multiplexing (WDM) is used to provide a more efficient use of the bandwidth of the optical fiber by allowing multiple users. For this thesis, a code division multiple access (CDMA) system using the heterodyne receiver

with DPSK and MFSK demodulation will be investigated. The benefits of using CDMA over WDM is that the multiple users share the entire channel's bandwidth and their access is asynchronous with no waiting or scheduling is involved. This receiver is a combination of coherent and noncoherent detection. The CDMA must be recovered coherently while the MFSK and DPSK is decoded noncoherently. The goal of this thesis is to perform a probability of bit error analysis for various signal-to-noise ratios, laser phase noise values, and multiple users.

The next chapter contains a description of the system. This includes a brief description of the components of the communication system, MFSK, MFSK-CDMA, DPSK, and DPSK-CDMA receivers as well as a discussion of the noise terms involved. Chapter III is an analysis of the MFSK and MFSK-CDMA systems with laser phase noise. Chapter IV is an analysis of the DPSK and DPSK-CDMA systems with laser phase noise. Chapter V contains the numerical results with the conclusions in Chapter VI.

II. SYSTEM DESCRIPTION

This chapter describes the proposed coherent optical heterodyne communication system. First, the basic coherent optical communication system is introduced including a discussion of the components involved. This is followed by a description of the proposed MFSK and MFSK-CDMA detectors and then a description of the DPSK and DPSK-CDMA detectors. Finally, the various noise terms present in the coherent optical heterodyne communication system are discussed.

A. SYSTEM COMPONENTS

The coherent optical heterodyne communication system proposed consists of an optical transmitter, a fiber optic transmission medium, and a receiver. The receiver is comprised of an optical mixer, a photodetector, and an IF demodulator. After the received signal is optically heterodyned and detected, further demodulation of the signal is performed electronically. A simple block diagram of this system is shown in Figure 1. A description of the system components follows, including the requirements imposed on the components for coherent optical communications.

1. Transmit Laser and Local Oscillator Laser

One of the challenges facing coherent optical heterodyne communications is the availability of single

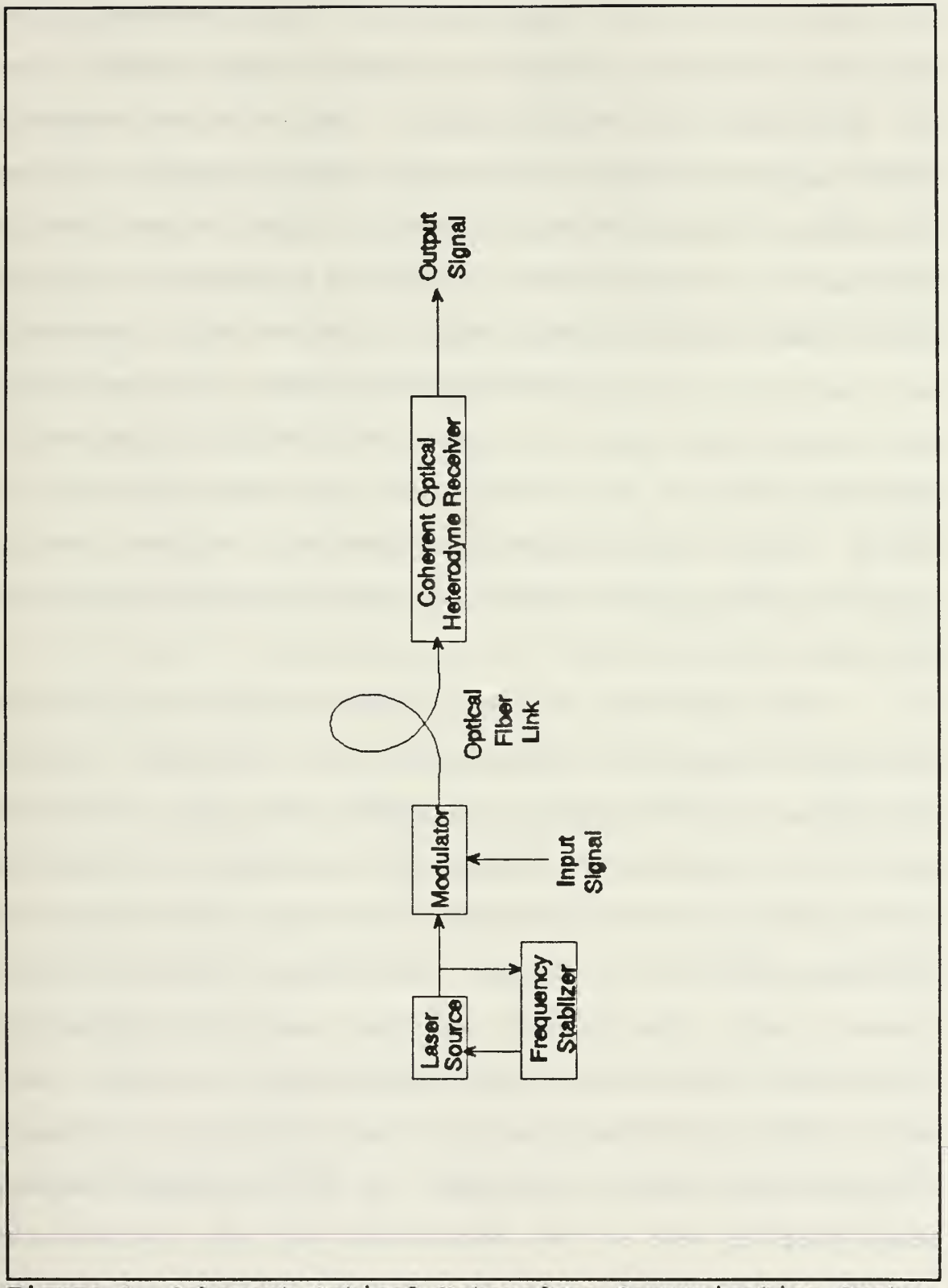

Figure 1 Coherent Optical Heterodyne Communication System

frequency lasers with high spectral purity and frequency stability. This requirement holds for both the transmit laser and the local oscillator laser. This stable frequency requirement eliminates the use of wideband sources such as incandescent light or other incoherent light sources such as light emitting diodes (LED's) which were used in early optical fiber communication systems. Gas lasers are also disregarded for practical systems due to size and safety considerations, even though HeNe lasers have been used in some experimental applications [Ref. 2]. This leaves semiconductor injection lasers as the obvious choice for both the transmit and the local oscillator laser due to its size and compatibility with electronic circuits.

In order for a semiconductor laser to meet the frequency stability requirements for coherent optical heterodyne communications, a feedback loop can be used to cancel any frequency variations in the laser. Distributed feedback lasers (DFB's) have been used to detect ASK and FSK noncoherently, i.e., envelope detection, without using a feedback path. The transmit and local oscillator lasers had linewidths 10 MHz and 50 MHz, respectively. Another scheme used to detect DPSK employed a DFB laser which had a linewidth reduction from 100 MHZ to 500 kHz due to an external feedback loop. [Ref. 2]

2. Modulator

Since high spectral purity is required from the sources, modulators that do not add noise to the signals are required. External modulators using lithium niobate (LiNbO) crystals have successfully been implemented for ASK, FSK, and PSK for bandwidths up to 30 GHz [Ref. 4:p. 431]. The LiNbO devices are electro-optic devices that modulate the optical wave based on an electric input signal.

3. Optical Fiber Link

Single mode or multimode fibers are the possible choices for the transmission medium for optical fiber communications. The single mode fiber has the major drawback of low coupling efficiency of the optical power from the source into the fiber because of its narrow diameter. The multimode fiber has the drawback of increased pulse spread and dispersion. The most important consideration for coherent optical communication systems is the ability to maintain polarity. This requirement directs the use of single mode fiber for the transmission medium of coherent optical communications.

The received signal and the local oscillator must be coaligned in linear polarization in order to achieve the maximum signal output for detection. One way that this polarization can be maintained is to use polarization-maintaining optical fibers as the transmission medium.

However, if a coherent optical heterodyne communication system is to be implemented on an existing optical fiber link that is not polarization-maintaining, then the polarities of the incoming signal and the local oscillator can be matched by use of polarization-diversity receivers or polarization controllers. Polarization matching is important for proper system operation but is beyond the scope of this thesis. The assumption will be made that the polarizations are matched for the proposed system so that the maximum signal energy is detected.

For a multiple random access scheme, several users transmit over the same optical fiber link. In order to implement this type of system, the different users' optical power must be combined at the transmitter outputs and subsequently split at the receiver inputs for each of the users. This can be achieved by the use of N/1 optical couplers and 1/N optical decouplers where N is the number of possible users that can have access to optical fiber link. WDM communication systems use this configuration, which is known as the broadband-multiplexing technique [Ref. 4:p. 395].

4. Receiver

The receiver of a coherent optical heterodyne communication system consists of an optical mixer, a photodetector, and an IF demodulator. A simple block diagram of this system is shown in Figure 2. The incoming optical

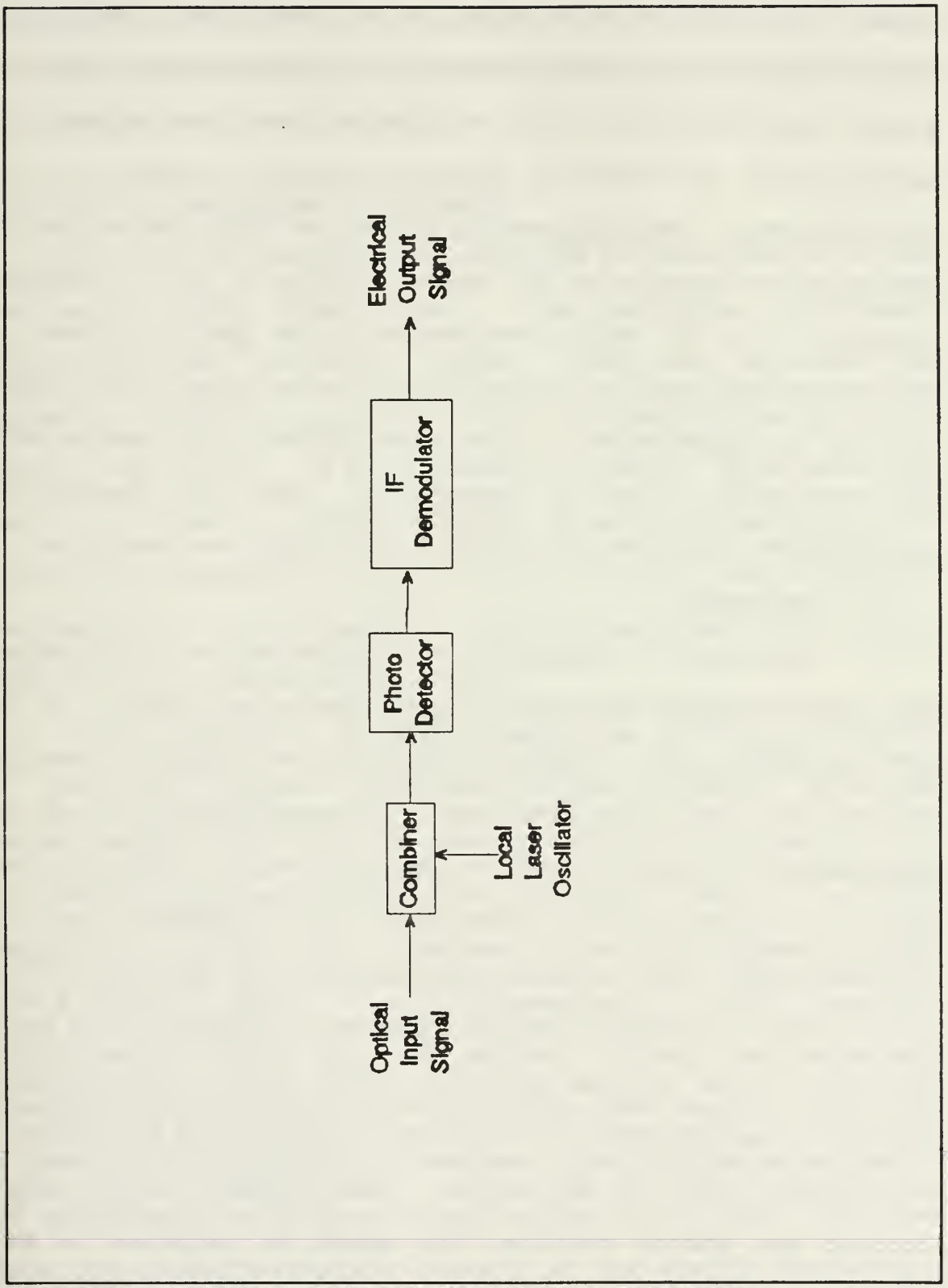

Figure 2 Coherent Optical Heterodyne Receiver

signal is combined, or mixed, with the local oscillator optical beam. The combiner ensures that the incoming optical signal beam and the local oscillator beam are matched in polarization to ensure a maximum signal strength at the photodetector. The combination of the two light beams form an interference pattern on the photodetector at the difference frequency, or IF, of the two beams. The optical signal is then converted from an optical signal to an electrical signal by the photodetector. Now, the signal is demodulated electronically by the IF demodulator. For this thesis, the noncoherent detection methods DPSK and MFSK are analyzed.

5. Detector

Two types of detectors are considered for this system: the PIN photodiode and the avalanche photodiode (APD). In the PIN photodiode, the incoming optical signal energy causes the release of free electrons into the conduction band of the semiconductor resulting in an output current. Ideally, each photon creates an electron-hole pair; however, due to recombination, the quantum efficiencies are less than 100%. In the APD, an incoming photon creates an electron-hole pair; but due to the intense electric field in the semiconductor material, more electron-hole pairs are generated resulting in an internal gain for the device. Even though a larger output current per photon results, the speed of response is much slower. Since the proposed coherent optical heterodyne

communication system to be examined in this thesis is a high data rate multiuser system, the PIN-FET photodiode shows the most promise [Ref. 5:p. 1296].

B. MFSK AND MFSK-CDMA DEMODULATOR

One of the IF demodulators analyzed in this thesis is the noncoherent MFSK demodulator. For multiple orthogonal signalling such as MFSK, several bits are selected to represent a symbol. A symbol is then transmitted as one of M possible waveforms. In 8-ary MFSK for example, three bits are chosen as a symbol, and one of eight possible frequencies are transmitted depending on the bit pattern and frequency assignments. The frequencies must be selected with proper separation to ensure orthogonality.

A block diagram of the MFSK demodulator is shown in Figure 3. The input to the demodulator is the IF output from the photodetector which results from the optical heterodyning of the incoming optical signal and the local laser. The MFSK demodulator consists of M branches of quadrature demodulators each matched to one of the M frequencies. Simpler receiver structures for MFSK such as matched filters and envelope detectors are not used since the MFSK-CDMA signal cannot be recovered with this type of receiver. Each of the branches of the quadrature demodulator mixes the incoming signal with in-phase and quadrature-phase signals at the branch frequency. The signals are then integrated and sampled over the symbol

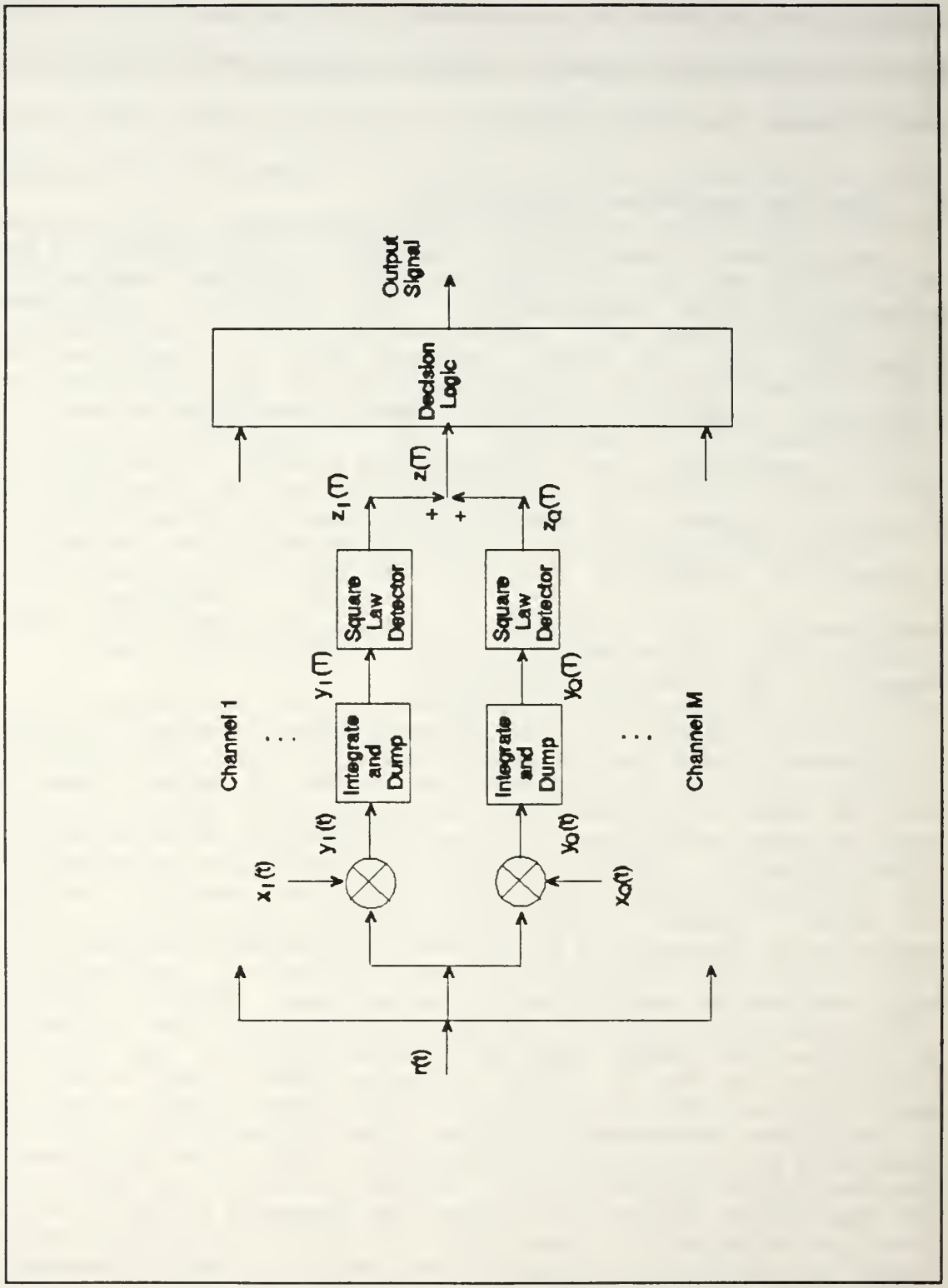

Figure 3 MFSK Demodulator (for an arbitrary channel i)

period. The in-phase and quadrature-phase components are then recombined at the output of the square law detector. If an incoming signal frequency is one of the M frequencies, then an output signal will be present in that branch. The other branches will only have noise present. The output of the M branches are then input to the decision logic which chooses the largest signal level and decodes the signal to a prescribed bit pattern.

The MFSK-CDMA demodulator differs from the MFSK demodulator in that it is a combination of both coherent and noncoherent demodulation schemes. The noncoherent demodulation of the MFSK is identical in both demodulator. The difference is that the user code that was used to spread the bit stream must be coherently demodulated. In order to recover the bit stream, the user sequence is modulated onto the local oscillator of the quadrature demodulator. The user sequence generated at the receiver must match that of the transmitter. Hence, coherent demodulation of the CDMA signal is required. An analysis of both the MFSK and MFSK-CDMA receivers is performed in the next chapter.

C. DPSK AND DPSK-CDMA DEMODULATOR

The second modulation scheme analyzed in this thesis is DPSK. For this communication scheme, each bit that is transmitted is encoded depending on its value and the value of the previous bit. The actual encoding scheme can be performed

in several different ways which are essentially variations of the description which follows. First, an initial code bit is assumed either a "0" or a "1". This code bit is then compared to the message bits that are to be transmitted. Each bit comparison results in a subsequent code bit. One method of creating the code bits is to allow the code bits to remain the same as long as the information bits match the code bits and change polarity when they do not match. The code bit sequence represents how the phase of the carrier is modulated. For example, a "0" code bit represents no phase shift and a "1" represents a 180° phase shift in the carrier.

Since two bits are compared in generating the code, then it seems at first glance that four combinations of bit patterns have to be detected at the receiver. This is not the case. Recovery of the DPSK signal is performed simply by noting whether or not a difference occurs between two subsequent bits. As long as the initial bit in the sequence is known, then the transmitted bit stream can be recovered.

The DPSK demodulator is shown in Figure 4. The upper channel of the demodulator has a signal present when a bit is the same as the previous bit transmitted. The lower channel has a signal present when a bit is different from the previous bit transmitted. The signals are first mixed with a local oscillator to break the incoming signal down into its in-phase and quadrature components. Next, the signals are delayed and the added/subtracted for the upper/lower channel in order to

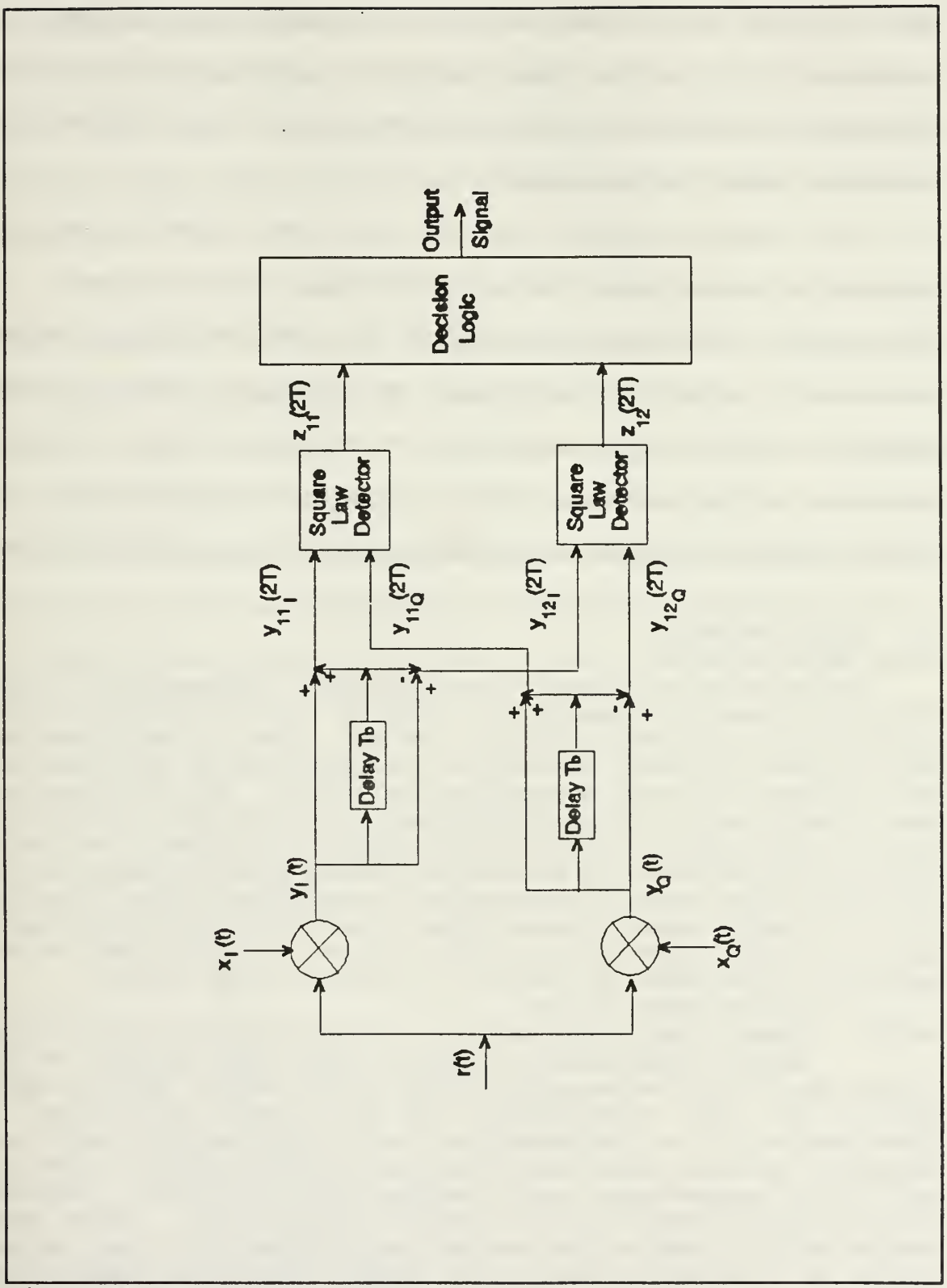

Figure 4 DPSK Demodulator

determine if the current and previous bits are the same or different. Finally the in-phase and quadrature-phase components are reconstituted by the square law detector to form the detection statistic.

In a manner similar to the MFSK-CDMA demodulator, the DPSK-CDMA demodulator is a combination of coherent and noncoherent detection. Once again the CDMA must be recovered coherently. This is achieved by applying the user code sequence to the local oscillator of the quadrature receiver. Once the bit stream is recovered from the chip sequence, the DPSK signal is demodulated noncoherently as described above.

D. NOISE SOURCES

The sources of noise are an important consideration in the analysis of any communication system. Just as important are the assumptions made regarding the noise. For the coherent optical heterodyne communication system with CDMA, four noise sources affect system performance: laser phase noise, receiver thermal noise, photodetector shot noise, and multiuser noise.

1. Laser Phase Noise

Since semiconductor lasers have been chosen as the source for the transmitter and the local oscillator of coherent optical communication system, laser phase noise can have a significant impact on system performance. Laser phase noise is a random process which occurs because of spontaneous emission within the laser cavity. This causes the phase of

the optical output wave to execute a random walk away from the value that it would have if spontaneous emission did not occur [Ref. 1:p. 2156]. This random phase process is evident by observing the broad linewidths of semiconductor laser emission spectrum.

The broad linewidth caused by laser phase noise on a laser transmitter or local oscillator has several effects. If the linewidth is large with respect to the signal frequency, then it is impossible to recover any timing or phase information from the signal. For example, for a homodyne detector where phase tracking is necessary, a linewidth on the order of 10 kHz is required for recovering information on a 100 Mbs system [Ref. 2:p. 11]. Also for high data rate systems and multiuser systems, an excessive linewidth limits the range of frequencies over which the transmit laser can be modulated. For optical heterodyne detection, the laser phase noise present in the system is the sum of the transmit laser's phase noise plus the local oscillator's phase noise.

Laser phase noise is caused by randomly occurring spontaneous emission events in the laser which cause sudden jumps in the phase of the electromagnetic field generated. The laser phase noise can be modelled as a random walk process. As the time between steps approaches zero, the random phase becomes a Brownian motion process characterized as a zero mean, white Gaussian process. The power spectral density of the laser phase noise is the integral over the

frequency band of operation of the Gaussian process which results in the Lorentzian spectrum. This can be determined experimentally by measuring the frequency fluctuations of the emitted light, or by observing the laser emission spectrum. The linewidth is determined by measuring the 3 dB bandwidth of the laser emission spectrum. [Ref. 1]

Even though the random walk process of the laser phase noise can be simulated in order to determine system performance, it rapidly becomes computationally prohibitive when the performance analysis is determined down to magnitudes of 10^{-9}. A closed form probability density function of a random variable that describes the effect of laser phase noise on the signal has been determined empirically by measuring the output envelope of various bandpass filters. A data rate of at least three times the laser linewidth is required in order for this probability density function to be valid.[Ref. 6] The laser phase noise models and the proposed data rates of operation will be discussed further in later sections.

2. Receiver Noise

Receiver noise that contributes to the degradation of the communication system is a combination of receiver thermal noise and photodetector shot noise. Thermal noise is shot noise that is generated in the resistive components of the receiver. Photodetector shot noise results from the fact that photons and electrons occur in discrete values. For coherent

heterodyne optical communication systems, a strong local oscillator is combined with the incoming optical signal. Since the number of events is increased for the shot noise process, then it can be assumed that the shot noise can be modelled as a zero mean, white Gaussian process. This allows both receiver noise terms to be combined and treated as a zero mean, white Gaussian noise process.[Ref. 1]

3. Multiuser noise

To improve multiple access for the coherent optical communication system, MFSK-CDMA and DPSK-CDMA are both considered. These methods make efficient use of the available bandwidth by providing asynchronous access to each user and by providing the entire bandwidth for each user's transmissions. Unlike other multiple access schemes that exist, CDMA has the advantage of no waiting and no collisions by the users. For CDMA, each user codes their transmissions to spread their signals over the available bandwidth. Ideally, each user code is orthogonal to all others, so each user is transparent to the others using the same bandwidth. In reality each user's receiver cross correlates some of the other users' signals. This interference due to other users is multiuser noise. Obtaining a mathematical relationship for the effect of multiuser noise in CDMA has been widely studied. In many cases, multiuser noise can be represented as a Gaussian random process. This assumption is valid as long as the spreading

code length and the number of users is large enough to invoke the central limit theorem.[Ref. 7] The MFSK-CDMA and DPSK-CDMA systems to be investigated are high data rate systems with long spreading codes to maximize the number of users.

III. ANALYSIS OF MFSK AND MFSK-CDMA

This chapter presents the probability of bit error analysis of the MFSK and the MFSK-CDMA systems. First, the conditional probability density function of the random variable that represents the decision statistic, Z_i, is derived. Then, the probability density function of the random variable that represents the effect of laser phase noise is introduced. This allows the determination of the probability of bit error for the MFSK system. The noise term that models the interference of the multiusers is then added to the analysis to obtain the probability of bit error for the MFSK-CDMA system.

A. The Conditional Probability Density Function of Z_i

The received signal, r(t), arriving at the input of the MFSK demodulator shown in Figure 3 results from the heterodyning of the transmitted optical signal with a local laser oscillator which is then converted to an electrical signal by the photodetector. This received signal is a combination of the signal and noise

$$r(t) = s_i(t) + n(t) \qquad (1)$$

where n(t) represents the receiver thermal noise and photodetector shot noise. This is assumed to be a zero mean,

white Gaussian process. The signal portion, $s_i(t)$, $i = 1, \ldots, M$, contains one of the orthogonal MFSK signals, and a random phase. The signals are assumed to be equally likely and have equal energy. The signal is represented as

$$s_i(t) = Re[b(t)\exp(j\omega_i t)] \tag{2}$$

where

$$b(t) = \sqrt{\frac{2E_s}{T_s}}\exp[j\theta(t)] \tag{3}$$

is the normalized complex baseband signal. The magnitude is normalized, with E_s as the symbol energy of the signal and T_s as the symbol period. The phase term, $\theta(t)$, is the composite phase noise due to the transmit and local oscillator lasers.

The received signal is multiplied by orthogonal signals to form the in-phase and quadrature components on each of the M channels. These signals form an orthonormal basis set and are matched to the frequency of that channel. The signals for an arbitrary jth channel are

$$x_{I_j}(t) = \sqrt{\frac{2}{T_s}}\cos(\omega_j t) \tag{4}$$

$$x_{Q_j}(t) = \sqrt{\frac{2}{T_s}}\sin(\omega_j t) \tag{5}$$

After the in-phase and quadrature components are formed, the received signal is then passed through an integrate and dump circuit. The random variables defined to represent the output of the integrate and dump circuit are

$$y_{I_i}(T_s) = \int_0^{T_s} r(t)\, x_{I_j}(t)\, dt \tag{6}$$

and

$$y_{Q_i}(T_s) = \int_0^{T_s} r(t)\, x_{Q_j}(t)\, dt \tag{7}$$

where j = 1, ..., M. For the case when i is not equal to j,

$$y_{I_i}(T_s) = n_I \,, \quad y_{Q_i}(T_s) = n_Q \,, \tag{8}$$

where n_I and n_Q are zero mean white Gaussian noise processes with variance $N_0/2$. When i = j,

$$y_{I_i}(T_s) = \frac{\sqrt{E_s}}{T_s} \int_0^{T_s} \cos\theta(t)\, dt + n_I \tag{9}$$

and

$$y_{Q_i}(T_s) = \frac{\sqrt{E_s}}{T_s} \int_0^{T_s} \sin\theta(t)\, dt + n_Q \tag{10}$$

The random variable that represents the detection statistic, Z_i, is formed by summing the output of the square law detectors of the two quadrature branches in each of the M channels shown in Figure 3. From the results in Equation (8),

the conditional probability density function for Z_i when i is not equal to j [Ref. 8:p. 109] is

$$p(z_j) = \frac{1}{2\sigma^2}\exp(-\frac{z_j}{2\sigma^2}) \tag{11}$$

When i = j, the conditional probability density function for Z_i is a noncentral Chi-squared distribution [Ref. 8:pp. 113-115]. Since

$$z_i(T_s) = [y_{I_i}(T_s)]^2 + [y_{Q_i}(T_s)]^2 \tag{12}$$

then by using Equation (9) and Equation (10), the conditional mean of the noncentral Chi-squared distribution is

$$\lambda = [\frac{\sqrt{E_s}}{T_s}\int_0^{T_s}\cos(\theta(t))\,dt]^2 + [\frac{\sqrt{E_s}}{T_s}\int_0^{T_s}\sin(\theta(t))\,dt]^2 \tag{13}$$

This is simplified to

$$\lambda = \frac{E_s}{T_s^2}\int_0^{T_s}|\exp[j\theta(t)]|^2 dt \tag{14}$$

If the random variable X [Ref. 9:p. 309] is defined such that

$$X = |\frac{1}{T_s}\int_0^{T_s}\exp[j\theta(t)]\,dt| \tag{15}$$

then the conditional mean for the Chi-squared distribution is

$$\lambda = E_s X^2 \tag{16}$$

With these results, the conditional probability density function of Z_i when i = j is

$$p(z_i,x) = \frac{1}{2\sigma^2}\exp[-\frac{z_i + E_s x^2}{2\sigma^2}]\, I_0[\frac{x\sqrt{E_s z_i}}{\sigma^2}] \qquad (17)$$

where I_0 is a zero order modified Bessel function of the first kind and $2\sigma^2$ is the variance of the additive white Gaussian noise [Ref. 8:p. 114]. This result is conditioned on X which results from the laser phase noise. This can be eliminated as shown

$$p(z_i) = \int_0^1 p(z_i|Z_i=z_i,x)\, p_X(x)\, dx \qquad (18)$$

B. Probability Density Function of X

As stated in Chapter II the laser phase noise is modelled as a random walk process from the value it has when no laser phase noise is present. A straightforward approach to evaluate the integral which defines the random variable X using Monte Carlo simulation has proven to be computationally intensive. Another approach to determine the probability density function of X has been to observe the output envelope of a bandpass filter. For a given impulse corrupted by laser phase noise, the filter response becomes a random process whose envelope at any instant in time is a random variable. This approach results in a closed form analytical solution for the probability density function of X by use of a curve fit

approximation to the actual probability density function. The probability density function of X used in this analysis is

$$p_X(x) = \alpha[1 - \exp(-\alpha)]^{-1}\exp[-\alpha(1 - x)] \quad \text{for } 0 \le x \le 1 \qquad (19)$$
$$= 0 \quad \text{otherwise}$$

where

$$\alpha = \frac{1.6}{\beta T_s}(1 + 0.5\sqrt{\beta T_s}) \qquad (20)$$

This probability density function assumes that an integrate and dump filter is used with rectangular signal pulses. In addition to the dependence on the filter type and the signalling chosen, the probability density function of X also depends on the laser linewidth, β, and the symbol period, T_s. [Ref. 6]

C. Probability of Bit Error for MFSK

The derivation of the probability of bit error for an MFSK system is developed by first finding the probability of correctly detecting a symbol. From this, the probability of symbol error is easily determined. The probability of symbol error is then converted to the probability of bit error. The analysis is performed by observing the statistics of the decision variable of an arbitrary channel. The decision variable, Z_i, results from the summation of the in-phase and quadrature branches of one of the M channels in the MFSK receiver as shown in Figure 3. As stated in Chapter II, the

MFSK receiver is corrupted by laser phase noise, receiver thermal noise, and photodetector shot noise.

For MFSK, the probability of correctly detecting symbol i is the probability that Z_i exceeds all the other decision statistics given that the symbol i was transmitted. Let P_c represent the probability of correctly detecting a symbol. Therefore,

$$P_c = P(Z_1 < Z_i \cap \cdots \cap Z_{i-1} < Z_i \cap Z_{i+1} < Z_i \cap \cdots \cap Z_M < Z_i) \qquad (21)$$

Rewriting in terms of the probability density function of Z_i, we have

$$P_c = \int_0^\infty P(Z_1 < Z_i, \ \ldots, \ Z_{i-1} < Z_i, \ Z_{i+1} < Z_i, \ \ldots, \ Z_M < Z_i \mid Z_i = z_i)\, p(z_i)\, dz_i \qquad (22)$$

Since each of the decision statistics are assumed to be independent, identically distributed random variables, the joint probability is rewritten as

$$P_c = \int_0^\infty [P(Z_j < Z_i)]^{M-1}\, p(z_i)\, dz_i \quad \text{where} \quad i \neq j \qquad (23)$$

This expression can be simplified further since

$$P(Z_j < Z_i) = \int_0^{z_i} p(z_j)\, dz_j \qquad (24)$$

Substituting Equation (11) and Equation (24) into Equation (23), we obtain

$$P_c = \int_0^{\infty} \left[\int_0^{z_i} \frac{1}{2\sigma^2}\exp\left(-\frac{z_j}{2\sigma^2}\right) dz_j\right]^{M-1} p(z_i)\, dz_i \qquad (25)$$

Evaluating the integral for z_j, we get

$$P_c = \int_0^{\infty} \left[1-\exp\left(-\frac{z_i}{2\sigma^2}\right)\right]^{M-1} p(z_i)\, dz_i \qquad (26)$$

Using the Binomial Expansion [Ref. 10:p. 347], we find the probability of correct detection as

$$P_c = \int_0^{\infty} \sum_{k=0}^{M-1} \binom{M-1}{k} (-1)^{k-1}\exp\left(-\frac{kz_i}{2\sigma^2}\right) p(z_i)\, dz_i \qquad (27)$$

Substituting Equation (17) into Equation (27), we get

$$P_c(x) = \int_0^{\infty} \frac{1}{2\sigma^2} \sum_{k=0}^{M-1} \binom{M-1}{k} (-1)^{k-1}\exp\left[-\frac{(k+1)z_i + E_s x^2}{2\sigma^2}\right] I_0\left(\frac{x\sqrt{E_s z_i}}{\sigma^2}\right) dz_i \qquad (28)$$

To obtain a workable expression for the probability of correct detection, the identity [Ref. 10:p. 404]

$$I_0\left(\frac{x\sqrt{E_s z_i}}{\sigma^2}\right) = \sum_{n=0}^{\infty} \left(\frac{x^2 E_s z_i}{4\sigma^4}\right)^n \left[\frac{1}{(n!)^2}\right] \qquad (29)$$

is substituted into Equation (28) to yield

$$P_c(x) = \int_0^{\infty} \frac{1}{2\sigma^2} \sum_{k=0}^{M-1} \binom{M-1}{k} (-1)^{k-1}\exp\left[-\frac{(k+1)z_i + E_s x^2}{2\sigma^2}\right] \sum_{n=0}^{\infty} \left(\frac{x^2 E_s z_i}{4\sigma^4}\right)^n \left[\frac{1}{(n!)^2}\right] dz_i \qquad (30)$$

After rearranging terms, we can express Equation (30) as

$$P_c(x) = \frac{1}{2\sigma^2}\exp\left(-\frac{E_s x^2}{2\sigma^2}\right) \sum_{k=0}^{M-1} \binom{M-1}{k} (-1)^{k-1} \sum_{n=0}^{\infty} \left(\frac{x^2 E_s}{4\sigma^4}\right)^n \left[\frac{1}{(n!)^2}\right] \int_0^{\infty} z_i^n \exp\left[\frac{(k+1)z_i}{2\sigma^2}\right] dz_i \qquad (31)$$

Next, use the definite integral [Ref. 10:p. 337]

$$\int_0^{\infty} z_i^n \exp\left[-\frac{(k+1)\,z_i}{2\sigma^2}\right] dz_i = \frac{n!}{\left[\frac{(k+1)}{2\sigma^2}\right]^{n+1}} \qquad (32)$$

in Equation (31) to get

$$P_c(x) = \frac{1}{2\sigma^2}\exp\left(-\frac{E_s x^2}{2\sigma^2}\right) \sum_{k=0}^{M-1} \binom{M-1}{k} (-1)^{k-1} \sum_{n=0}^{\infty} \left(\frac{x^2 E_s}{4\sigma^4}\right)^n \left[\frac{1}{(n!)^2}\right] \left[\frac{n!}{\left(\frac{(k+1)}{2\sigma^2}\right)^{n+1}}\right] \qquad (33)$$

which can be simplified to

$$P_c(x) = \frac{1}{2\sigma^2}\exp\left(-\frac{E_s x^2}{2\sigma^2}\right) \sum_{k=0}^{M-1} \binom{M-1}{k} (-1)^{k-1} \sum_{n=0}^{\infty} \left(\frac{x^2 E_s}{2\sigma^2}\right)^n \left[\frac{1}{(n!)}\right] \left[\frac{1}{(k+1)^{n+1}}\right] \qquad (34)$$

Finally, the expression

$$\sum_{n=0}^{\infty} \frac{1}{n!} \left[\frac{x^2 E_s}{(k+1)\,(2\sigma^2)}\right]^n = \exp\left[\frac{x^2 E_s}{(k+1)\,(2\sigma^2)}\right] \qquad (35)$$

is used in Equation (34) to obtain the probability of correctly detecting a symbol

$$P_c(x) = \exp\left(-\frac{E_s x^2}{2\sigma^2}\right) \sum_{k=0}^{M-1} \binom{M-1}{k} (-1)^{k-1} \frac{1}{(k+1)} \exp\left[\frac{x^2 E_s}{(k+1)\,(2\sigma^2)}\right] \qquad (36)$$

This is simplified further to

$$P_c(x) = \sum_{k=0}^{M-1} \binom{M-1}{k} (-1)^{k-1} \frac{1}{(k+1)} \exp\left[-\frac{k x^2 E_s}{(k+1)\,(2\sigma^2)}\right] \qquad (37)$$

The probability of symbol error is easily found from the probability of correctly detecting a symbol as

$$P_s(x) = 1 - P_c = \sum_{k=1}^{M-1} \binom{M-1}{k} (-1)^{k-1} \frac{1}{(k+1)} \exp\left[-\frac{k x^2 E_s}{(k+1)\,(2\sigma^2)}\right] \qquad (38)$$

The dependence on the random variable, X, is removed by averaging as follows

$$P_s = \int_0^1 \sum_{k=1}^{M-1} \binom{M-1}{k} (-1)^{k-1} \frac{1}{(k+1)} \exp\left[-\frac{kx^2 E_s}{(k+1)(2\sigma^2)}\right] p_X(x)\, dx \quad (39)$$

In order to compare the system performance of this system with other digital communication systems the signal to noise ratio is expressed in terms of E_b and N_0. If we substitute

$$\sigma^2 = \frac{N_o}{2} \quad , \quad E_s = E_b \log_2 M, \quad (40)$$

into the above, then the probability of symbol error becomes

$$P_s = \int_0^1 \sum_{k=1}^{M-1} \binom{M-1}{k} (-1)^{k-1} \frac{1}{(k+1)} \exp\left[-\frac{kx^2 E_b \log_2 M}{(k+1) N_o}\right] p_X(x)\, dx \quad (41)$$

The probability of symbol error is converted into the probability of bit error by [Ref. 11:p. 180]

$$P_b = \left[\frac{M}{2(M-1)}\right] P_s \quad (42)$$

so that performance comparisons can be made with binary communication systems. This results in the final expression for the probability of bit error that is used in the numerical analysis

$$P_b = \int_0^1 \left[\frac{M}{2(M-1)}\right] \sum_{k=1}^{M-1} \binom{M-1}{k} (-1)^{k-1} \frac{1}{(k+1)} \exp\left[-\frac{kx^2 E_b \log_2 M}{(k+1) N_o}\right] p_X(x)\, dx \quad (43)$$

As a check, let the laser phase noise become negligible. Hence,

$$p_X(x) \approx \delta(x-1) \tag{44}$$

Evaluating the integral in Equation (43), we get the probability of bit error

$$P_b = \left[\frac{M}{2(M-1)}\right] \sum_{k=1}^{M-1} \binom{M-1}{k} (-1)^{k-1} \frac{1}{(k+1)} \exp\left[-\frac{kE_b \log_2 M}{(k+1)N_o}\right] \tag{45}$$

which compares to the probability of bit error for noncoherent MFSK detection [Ref. 11:p. 177]. For M = 2, the probability of bit error reduces to

$$P_b = \frac{1}{2} \exp\left(-\frac{E_b}{2N_o}\right) \tag{46}$$

which corresponds to the probability of bit error expression for noncoherent binary FSK [Ref. 11:p. 166]. The performance of the MFSK-CDMA system is analyzed next by adding the noise contributed by multiple users.

D. Probability of Bit Error for MFSK-CDMA

The MFSK-CDMA system allows multiple users asynchronous access to the same channel. Ideally, each user will have use of the channel with no interference from the other users. In order to accomplish this, each user is assigned a code which is used to modulate the carrier for each symbol that is transmitted. The codes are ideally chosen to be orthogonal so that only a particular user's code is demodulated at a particular receiver. In a practical system, pseudo-noise

codes generated from m-sequences or Gold codes, obtained by the modulo-2 sum of two m-sequences, are used. Some cross correlation noise occurs between the various users' when these codes are used, and this degrades system performance.

The difference between the MFSK receiver and the MFSK-CDMA receiver is that the user's code is applied to the transmit message. This causes the received signal from Equation (2) to become

$$s_i(t) = Re[a(t)b(t)\exp(j\omega_i t)] \tag{47}$$

where a(t) is the user code sequence. At the receiver, the user's code must also be applied to the in-phase branch multiplier from Equation (4)

$$x_{I_i}(t) = \sqrt{\frac{2}{T_s}}a(t)\cos(\omega_i t) \tag{48}$$

and the quadrature branch multiplier from Equation (5)

$$x_{Q_i}(t) = \sqrt{\frac{2}{T_s}}a(t)\sin(\omega_i t) \tag{49}$$

for each channel. The user code sequence at the receiver must be synchronized to the transmitter's user code, therefore requiring coherent detection of the code sequence. After this is performed, the signal is noncoherently detected by the MFSK demodulator as previously discussed.

The multiple user noise model used in this analysis is derived for asynchronous MFSK detection where random signature

sequences are used. Random signature sequences are not physically realizable but are used in mathematical analysis to simplify the noise expression due to the multiple users. It has been demonstrated that random sequences and Gold codes yield comparable performance [Ref. 12:p. 598]. For the model used it is assumed that the user's transmission are not synchronized, that the user's transmit at equal power, and that the data streams, time delays, and phase shifts are mutually independent random variables.

The average probability of bit error for MFSK-CDMA is approximated by using a zero mean, white Gaussian noise random variable for the multiple access interference. The noise variance is [Ref. 7:p. 692]

$$\sigma^2 = \frac{N_0}{2} + \frac{(K-1)E_s}{3MN'} \qquad (50)$$

where $N_0/2$ is the two-sided power spectral density of the additive white Gaussian receiver discussed previously, E_s is the symbol energy, M is the order of signalling, K is the number of users, and N' is the length of the spreading code.

IV. ANALYSIS OF DPSK AND DPSK-CDMA

This chapter develops the probability of bit error for the DPSK and DPSK-CDMA systems. The conditional probability density function of the decision statistic is derived first. The probability density function of the laser phase noise is then restated noting the differences with that which was used for the MFSK case. Finally, the probability of bit error is developed for the DPSK system. The multiuser noise is then added to the analysis resulting in the probability of bit error for DPSK-CDMA.

A. Conditional Probability Density Function of Z_{11} and Z_{12}

Similar to the MFSK case, the received signal, r(t), at the input of the DPSK demodulator is the result of the heterodyning of the optical signals from the transmit laser and the local oscillator laser as shown in Figure 4. The received signal is a combination of the signal and noise

$$r(t) = s(t) + n(t) \tag{51}$$

where n(t) represents the receiver thermal noise and photodetector shot noise. This is assumed to be a zero mean, white Gaussian process. The signal portion, s(t), contains an IF frequency whose phase is modulated based on the coding scheme described in Chapter II. The signals are assumed to be

equally likely and have equal energy. The signal is represented as

$$s(t) = Re[b(t)\exp(j\omega t)] \tag{52}$$

where

$$b(t) = \sqrt{\frac{2E_b}{T_b}}\exp[j(\theta(t) + \phi(t))] \tag{53}$$

is the normalized complex baseband signal corrupted by laser phase noise. The magnitude is normalized with E_b, the energy transmitted per bit, and T_b, the bit period. The phase term, $\theta(t)$, is used to represent the combined laser phase noise due to the transmit laser and the local oscillator laser. The phase term, $\phi(t)$, represents the encoding performed on the bit stream prior to transmission. The possible values of $\phi(t)$ are $\{0,\pi\}$.

The demodulation of the DPSK signal begins by first multiplying the received signals with those of an orthonormal basis set. This multiplication of the signals is performed electronically by a mixer which translates the signal from IF to baseband and forms the in-phase and quadrature components of the complex baseband signal. The mixing waveforms are

$$x_I(t) = \sqrt{\frac{2}{T_b}}\cos(\omega T) \tag{54}$$

and

$$x_Q(t) = \sqrt{\frac{2}{T_b}} \sin(\omega T) . \tag{55}$$

After mixing, the received signal passes through an integrate and dump circuit. The random variables defined to represent the output of the integrate and dump circuit are

$$y_I(T_b) = \int_0^{T_b} r(t) x_I(t)\, dt \tag{56}$$

and

$$y_Q(T_b) = \int_0^{T_b} r(t) x_Q(t)\, dt \tag{57}$$

Substituting Equation (51), (52), and (53) into Equations (56) and (57) and simplifying, we obtain

$$y_I(T_b) = \frac{\sqrt{E_b}}{T_b} \int_0^{T_b} \cos[\theta(t) + \phi(t)]\, dt + n_I(T_b) \tag{58}$$

and

$$y_Q(T_b) = -\frac{\sqrt{E_b}}{T_b} \int_0^{T_b} \sin[\theta(t) + \phi(t)]\, dt + n_Q(T_b) \tag{59}$$

where n_I and n_Q are zero mean, white Gaussian noise processes with variance $\sigma^2 = N_0/2$. Since $\phi(t)$ can only take on the discrete values $\{0,\pi\}$, then Equations (58) and (59) can be rewritten as

$$y_I(T_b) = \frac{\sqrt{E_b}}{T_b} \int_0^{T_b} \cos[\theta(t)]\cos[\phi(t)]\,dt + n_I(T_b) \qquad (60)$$

and

$$y_Q(T_b) = -\frac{\sqrt{E_b}}{T_b} \int_0^{T_b} \sin[\theta(t)]\cos[\phi(t)]\,dt + n_Q(T_b) \qquad (61)$$

The next step in the demodulation of DPSK for the receiver shown in Figure 4 is the formation of four signals represented by the random variables: $y_{11I}(2T_b)$, $y_{11Q}(2T_b)$, $y_{12I}(2T_b)$, and $y_{12Q}(2T_b)$. As discussed in Chapter II, only two cases are needed for the DPSK detection: when the message bit is the same polarity as the previous message bit and when they have different polarities. The signals in the upper channel, the 11 case, are represented by the random variables, $y_{11I}(2T_b)$ and $y_{11Q}(2T_b)$, each with a nonzero mean when adjacent message bits are the same. The signals in the lower branch, the 12 case, are represented by the random variables, $y_{12I}(2T_b)$ and $y_{12Q}(2T_b)$, each with a nonzero mean when adjacent message bits are different. Otherwise, the signals in each channel are represented by zero mean random variables since only noise is present. For example, only noise will be present in the lower channel when the adjacent bits are the same, the 11 case. This case is now developed.

The upper branch inputs to the square law detector in Figure 4, $y_{11I}(2T_b)$ and $y_{11Q}(2T_b)$, are formed by adding the

output of the integrate and dump circuit for two adjacent bit intervals. For the in-phase component,

$$y_{11_I}(2T_b) = y_I(T_b) + y_I(2T_b) \tag{62}$$

can be rewritten using the results from Equation (60) as

$$y_{11_I}(2T_b) = \frac{\sqrt{E_b}}{T_b}\int_0^{T_b}\cos\theta(t)\cos\phi(t)\,dt + n_I(T_b) + \frac{\sqrt{E_b}}{T_b}\int_{T_b}^{2T_b}\cos\theta(t)\cos\phi(t)\,dt + n_I(2T_b) \tag{63}$$

The sum of the two noise random variables results in a zero mean white Gaussian process with variance $2\sigma^2$ since the noise is assumed to be an independent, identically distributed, stationary Gaussian process. The adjacent bits are assumed to have the same polarity, therefore $\cos[\phi(t)]$ has the same value over both bit intervals, either both +1 or -1. Also, since $\theta(t)$ is an independent, identically distributed Brownian motion process, then the expression for $y_{11_I}(2T_b)$ can be rewritten as

$$y_{11_I}(2T_b) = \pm\frac{2\sqrt{E_b}}{T_b}\int_0^{T_b}\cos\theta(t)\,dt + n_I^* \tag{64}$$

where n_I^* is a zero mean, white Gaussian noise process with variance $2\sigma^2$ discussed previously. Similarly, the quadrature component for the 11 case can be written as

$$y_{11_Q}(2T_b) = \pm \frac{2\sqrt{E_b}}{T_b} \int_0^{T_b} \sin\theta(t)\,dt + n_Q^* \tag{65}$$

where n_Q^* is a zero mean, white Gaussian noise process with variance $2\sigma^2$. Note that the signs of Equations (64) and (65) have no significance since they are input into a square law detector. Therefore, the sign is dropped from further analysis.

The lower branch inputs to the square law detector, y_{12I} and y_{12Q}, are formed by subtracting the output of the integrate and dump circuit for two adjacent bit intervals. For the in-phase component this becomes

$$y_{12_I}(2T_b) = y_I(T_b) - y_I(2T_b) \tag{66}$$

which can be rewritten using the results from Equation (60) as

$$\begin{aligned} y_{12_I}(2T_b) = {} & \frac{\sqrt{E_b}}{T_b} \int_0^{T_b} \cos\theta(t)\cos\phi(t)\,dt + n_I(T_b) - \\ & \frac{\sqrt{E_b}}{T_b} \int_{T_b}^{2T_b} \cos\theta(t)\cos\phi(t)\,dt - n_I(2T_b) \end{aligned} \tag{67}$$

The difference of the two noise random variables results in a zero mean white Gaussian process with variance $2\sigma^2$. This is true since the noise is assumed to be an independent, identically distributed, stationary Gaussian process. The adjacent bits are assumed to have the same polarity, and $\theta(t)$ is an independent identically distributed Brownian motion process. Therefore, the integrals subtract out resulting in

$$y_{12_I}(2T_b) = n_I^* \tag{68}$$

where n_I^* is a zero mean, white Gaussian noise process with variance $2\sigma^2$. Similarly, the quadrature component can be written as

$$y_{12_Q}(2T_b) = n_Q^* \tag{69}$$

where n_Q^* is a zero mean, white Gaussian noise process with variance $2\sigma^2$.

The detection statistics, Z_{11} and Z_{12}, are formed by summing the outputs of the square law detector of the in-phase and quadrature components for each case. Since the outputs of the square law detectors for the 12 case are zero mean white Gaussian noise processes, Equation (68) and (69), then the conditional probability density function for Z_{12} is [Ref. 8:p. 109]

$$p(z_{12}) = \frac{1}{4\sigma^2}\exp(-\frac{z_{12}}{4\sigma^2}) \tag{70}$$

The decision statistic, Z_{11}, is formed by Gaussian random variables with non-zero mean. Therefore, the conditional probability density function for Z_{11} is written as a non-central Chi-squared distribution [Ref. 8:p. 113-115]. Since

$$z_{11}(2T_b) = [y_{11_I}(2T_b)]^2 + [y_{11_Q}(2T_b)]^2 \tag{71}$$

then the conditional mean of the noncentral Chi-squared distribution is

$$\lambda = [\frac{2\sqrt{E_b}}{T_b}\int_0^{T_b}\cos(\theta(t))\,dt]^2 + [\frac{2\sqrt{E_b}}{T_b}\int_0^{T_b}\sin(\theta(t))\,dt]^2 \quad (72)$$

This can be simplified to

$$\lambda = \frac{4E_b}{T_b^2}\int_0^{T_b}|\exp[j\theta(t)]\,dt|^2 dt \quad (73)$$

If the random variable X [Ref. 9:p. 309] is defined such that

$$X = |\frac{1}{T_b}\int_0^{T_b}\exp[j\theta(t)]\,dt| \quad (74)$$

then the conditional mean of the noncentral Chi-squared distribution is

$$\lambda = 4E_bX^2 \quad (75)$$

The conditional probability density function of Z_{11} is

$$p(z_{11},x) = \frac{1}{4\sigma^2}\exp[-\frac{z_{11} + 4E_bx^2}{4\sigma^2}]\,I_0[\frac{x\sqrt{E_bz_{11}}}{2\sigma^2}] \quad (76)$$

where I_0 is a zero order modified Bessel function of the first kind and $\sigma^2 = N_0/2$ is the two sided power spectral density of the white Gaussian noise [Ref. 9:p. 114]. This result is also conditioned on X, which is determined by the laser phase noise. The conditioning on X is eliminated as shown

$$p(z_{11}) = \int_0^1 p(z_{11},x)\,p_X(x)\,dx \quad (77)$$

B. Probability Density Function of X

The model used for the probability density function of the random variable, X, for this analysis is the same as that which was introduced in Chapter III. The difference between this expression and that of Equations (19) and (20) is the expression for α. For MFSK, the integration occurs over the symbol period, T_s, compared to T_b for the DPSK demodulator. Therefore, the probability density function of X used for the DPSK and DPSK-CDMA analysis is

$$\begin{aligned} p_X(x) &= \alpha[1 - \exp(-\alpha)]^{-1}\exp[-\alpha(1 - x)] \quad \textit{for } 0 \le x \le 1 \\ &= 0 \quad \textit{otherwise} \end{aligned} \tag{78}$$

where

$$\alpha = \frac{1.6}{\beta T_b}(1 + 0.5\sqrt{\beta T_b}) \tag{79}$$

This probability density function of X assumes that an integrate and dump filter is used with rectangular signal pulses. The probability density function of X also depends on the laser linewidth, β, and the bit period, T_b. [Ref. 6]

C. Probability of Bit Error for DPSK

The average probability of obtaining a bit error depends on the probability of detecting the 11 case when the 12 case is transmitted plus the probability of detecting the 12 case when the 11 case is transmitted. This is expressed mathematically as

$$P_b = P(Z_{11}|H_{12})\,P(H_{12}) + P(Z_{12}|H_{11})\,P(H_{11}) \qquad (80)$$

where H_{11} and H_{12} are the hypotheses that case 11 or 12 is transmitted, respectively. Assuming equally likely signalling, we have $P(H_{11}) = P(H_{12}) = 1/2$. Also, using the assumption that the probability of making an error is the same for either case, we get

$$P_b = \frac{1}{2}P(Z_{11}|H_{12}) + \frac{1}{2}P(Z_{12}|H_{11}) = P(Z_{12}|H_{11}) \qquad (81)$$

The probability of bit error is now expressed using the conditional probability density functions derived in the previous section. The probability of bit error is

$$P_b = \int_0^\infty Pr[Z_{12} > Z_{11}]\,p(z_{11})\,dz_{11} \qquad (82)$$

Knowing that

$$Pr(Z_{12} > Z_{11}) = \int_{z_{11}}^\infty p(z_{12})\,dz_{12} \qquad (83)$$

and substituting this and Equation (70) into Equation (82), we obtain

$$P_b = \int_0^\infty \left[\int_{z_{11}}^\infty \frac{1}{4\sigma^2}\exp\left(-\frac{z_{12}}{4\sigma^2}\right)dz_{12}\right]\,p(z_{11})\,dz_{11} \qquad (84)$$

Evaluating the inner integral and substituting Equation (76) into the result, we obtain

$$P_b(x) = \int_0^\infty \exp\left(-\frac{z_{11}}{4\sigma^2}\right) \frac{1}{4\sigma^2} \exp\left(-\frac{z_{11} + 4E_b x^2}{4\sigma^2}\right) I_0\left(\frac{x\sqrt{E_b z_{11}}}{\sigma^2}\right) dz_{11} \quad (85)$$

This expression can be rewritten

$$P_b(x) = \int_0^\infty \frac{1}{4\sigma^2} \exp\left(-\frac{2z_{11} + 4E_b x^2}{4\sigma^2}\right) I_0\left(\frac{x\sqrt{E_b z_{11}}}{\sigma^2}\right) dz_{11} \quad (86)$$

The identity [Ref. 10:p. 404],

$$I_0\left(\frac{x\sqrt{E_b z_{11}}}{\sigma^2}\right) = \sum_{n=0}^{\infty} \left(\frac{x^2 E_b z_{11}}{4\sigma^4}\right)^n \left[\frac{1}{(n!)^2}\right] \quad (87)$$

is substituted into Equation (86) to obtain

$$P_b(x) = \frac{1}{4\sigma^2} \exp\left(-\frac{4E_b x^2}{4\sigma^2}\right) \sum_{n=0}^{\infty} \left(\frac{x^2 E_b}{4\sigma^4}\right)^n \frac{1}{(n!)^2} \int_0^\infty \exp\left(\frac{z_{11}}{2\sigma^2}\right) z_{11}^n \, dz_{11} \quad (88)$$

In order to further simplify the expression, the definite integral [Ref. 10:p. 337]

$$\int_0^\infty z_{11}^n \exp\left(\frac{z_{11}}{2\sigma^2}\right) dz_{11} = \frac{n!}{\left(\frac{1}{2\sigma^2}\right)^{n+1}} \quad (89)$$

is used in Equation (88) and the probability of bit error becomes

$$P_b(x) = \frac{1}{2} \exp\left(-\frac{E_b x^2}{\sigma^2}\right) \sum_{n=0}^{\infty} \left(\frac{x^2 E_b}{2\sigma^2}\right) \frac{1}{n!} \quad (90)$$

Since [Ref. 10:p. 349]

$$\sum_{n=0}^{\infty} \left(\frac{x^2 E_b}{2\sigma^2}\right) \frac{1}{n!} = \exp\left(\frac{x^2 E_b}{2\sigma^2}\right) \tag{91}$$

then

$$P_b = \frac{1}{2}\exp\left(-\frac{E_b x^2}{\sigma^2}\right) \exp\left(\frac{x^2 E_b}{2\sigma^2}\right) = \frac{1}{2}\exp\left(-\frac{x^2 E_b}{2\sigma^2}\right) \tag{92}$$

The final form of the probability of bit error for DPSK is found by removing the conditioning on X and letting $\sigma^2 = N_0/2$ so that the probability of bit error is expressed in terms of E_b and N_0. This results in

$$P_b(x) = \int_0^1 \frac{1}{2}\exp\left(-\frac{x^2 E_b}{N_0}\right) p_X(x)\, dx \tag{93}$$

If the laser phase noise is allowed to become negligible, then

$$p_X(x) = \delta(x-1) \tag{94}$$

and

$$P_b = \frac{1}{2}\exp\left(-\frac{E_b}{N_0}\right) \tag{95}$$

This result corresponds to the probability of bit error for conventional DPSK communication systems [Ref. 11:p. 166]. Next, the performance of the DPSK-CDMA is analyzed by adding the noise contributed by multiple users.

D. Probability of Bit Error for DPSK-CDMA

The DPSK-CDMA system allows multiple users asynchronous access to the same channel. Ideally, each user transmits and receives on the channel with no interference from the other users. This is achieved by assigning a code to each user which is used to modulate the phase of the carrier for each bit that is transmitted. The codes are ideally chosen to be orthogonal so that only the user's code is demodulated at the receiver. In a practical system, pseudo-noise codes generated from m-sequences or Gold codes, obtained by the modulo-2 sum of two m-sequences, are used. When used, these codes result in some cross correlation noise in the receiver from other users' codes. This degrades system performance. Obviously, system performance worsens as the number of users increase.

The difference between the DPSK receiver and the DPSK-CDMA receiver is that the user's code is applied to the transmit message. This causes the received signal from Equation (52) to become

$$s(t) = Re[a(t)b(t)\exp(j\omega t)] \tag{96}$$

where a(t) is the user code sequence. At the receiver, the user's code must also be applied to the in-phase branch multiplier from Equation (54)

$$x_I(t) = \sqrt{\frac{2}{T_b}}a(t)\cos(\omega t) \tag{97}$$

and the quadrature branch multiplier from Equation (55)

$$x_Q(t) = \sqrt{\frac{2}{T_b}} a(t) \sin(\omega t) \qquad (98)$$

The user code sequence at the receiver must be synchronized to the transmitter's code sequence. This requires coherent detection of the code sequence. After the code sequence is properly demodulated, then the signal is noncoherently demodulated by the DPSK receiver discussed previously.

The model used for the multiple user interference for this analysis is derived solely for DPSK detection using random signature sequences. Several assumptions are made for this model. First, the various users' transmissions are not synchronized. Second, the users transmit with equal power in the channel. Finally, the data streams, time delays, and phase shifts are assumed to be mutually independent random variables.

The average probability of bit error for DPSK-CDMA is approximated by using a zero mean, Gaussian noise random variable for the multiple access interference. The noise variance is [Ref. 7:p. 692]

$$\sigma^2 = \frac{N_0}{2} + \frac{2(K-1)E_b}{3N} \qquad (99)$$

The term, $N_0/2$, is the two sided power spectral density of the additive white Gaussian receiver noise discussed previously.

The term, E_b, is the average bit energy. The number of users of the system is K, and the codelength implemented is N.

V. NUMERICAL RESULTS

For the single user implementation of the coherent optically heterodyned communication systems, numerical results are obtained by evaluating the probability of bit error as a function of E_b/N_0 for various βT_s or βT_b values. The probability of bit error is the standard method of expressing communication system performance, even when M-ary signalling is used. The probability of bit error is expressed as a function of E_b/N_0 rather than the signal to noise ratio (SNR) in order to facilitate the comparison of one digital communication system to another. The product of the laser linewidth and the symbol period, βT_s, for MFSK or the product of the laser linewidth and the bit period, βT_b, for DPSK is also used as a parameter for the evaluation of the probability of bit error for MFSK and DPSK systems, respectively, when corrupted by laser phase noise. In order to simplify the discussion, the product of the laser linewidth and the time period of integration will henceforth be referred to as βT for both systems. This product allows the data rate of the system, inverse of the time period of integration, to be expressed in terms of the laser linewidth. A higher data rate results in a lower βT for a given laser linewidth. This yields general results that do not depend on a specific transmit laser or local oscillator laser.

For the multiple user implementation of the coherent optical communication system, numerical results are obtained by evaluating the probability of bit error for various number of users, various codelengths, and a particular βT. Changing the number of users of the system affects the amount of noise that is present in the system. This is analogous to varying E_b/N_0. A maximum value of 16 dB is chosen for E_b/N_0 for all of the systems analyzed. This yields a probability of bit error of 10^{-9} for the M = 2, or binary, FSK case. This value is chosen to anchor the comparisons of the probability of bit error calculations of the MFSK and DPSK systems. For the multiple user analysis, it is assumed that the optical signal power is normalized to unity and that each user's transmit power is balanced in the combined signal of the optical channel.

All of the numerical analyses performed in this thesis require numerical integration to obtain the probability of bit error. This is performed using MATLAB. The results for MFSK, MFSK-CDMA, DPSK, and DPSK-CDMA are presented next.

A. Multiple Frequency-Shift Keying

The probability of bit error for conventional MFSK is computed first in order to obtain a reference for the probability of bit error for the coherent optically heterodyned MFSK system. Equation (45) is evaluated for various E_b/N_0 and is plotted in Figure 5. The five cases of

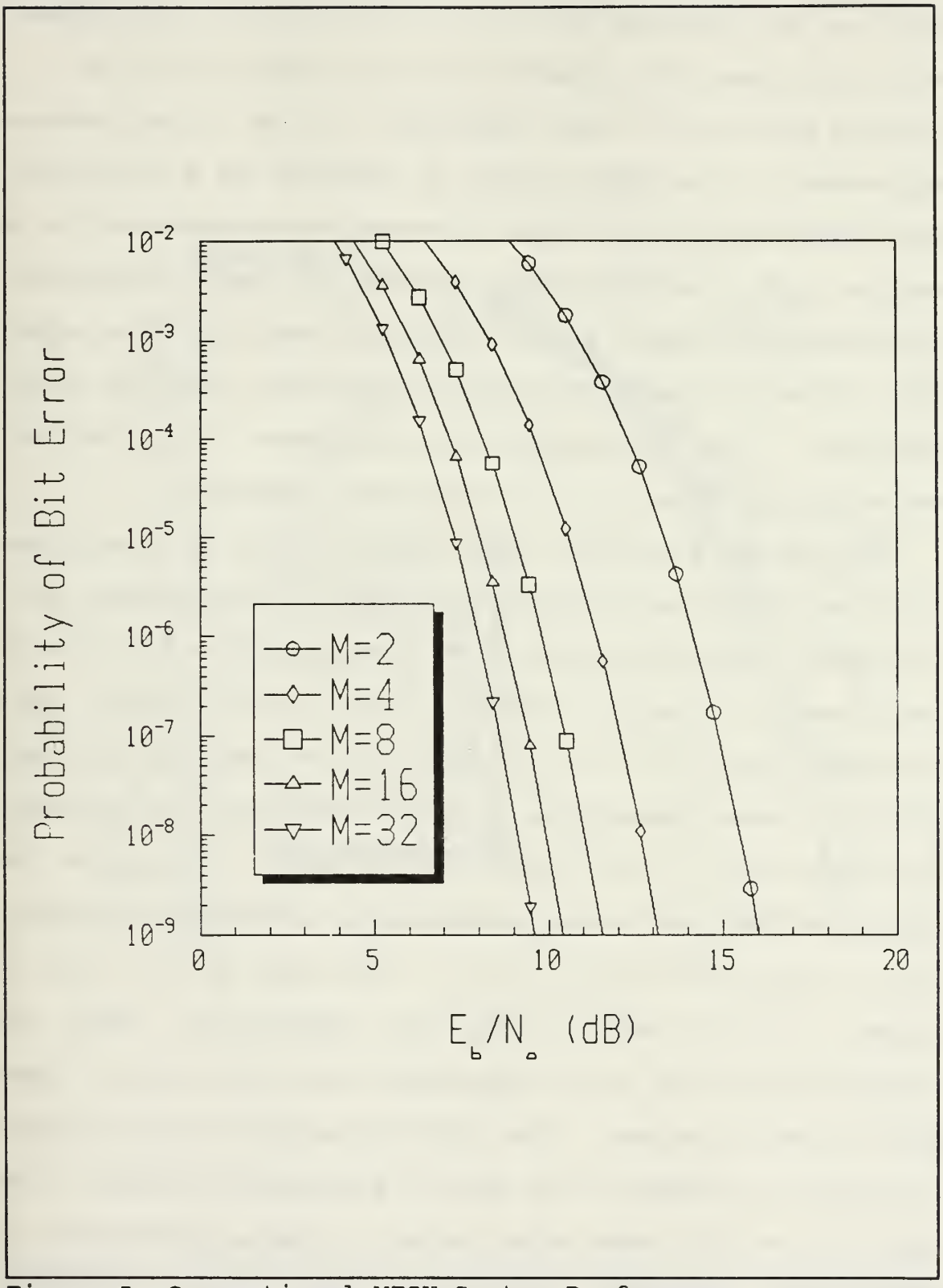

Figure 5 Conventional MFSK System Performance

MFSK that are analyzed (M = 2, 4, 8, 16, and 32) are shown. From this figure the probability of bit error of 10^{-9} is obtained for the M = 2 case when E_b/N_0 = 16 dB. A performance improvement of the MFSK system is observed as M increases. This improvement occurs since the systems are compared for a constant E_b/N_0. As the number of bits per symbol increases, the transmitted signal energy increases resulting in a higher SNR. Obviously, the performance of the system improves as SNR increases. This improvement in performance as M increases occurs at the expense of requiring more bandwidth.

Each of the five MFSK cases when corrupted by laser phase noise are calculated by numerically integrating Equation (43). Each MFSK case with values of βT that vary from 0.1 to 0.01 are shown in Figure 6 through 10. As the symbol rate increases from βT = 0.1 to 0.01, it is observed that the effect of laser phase noise is less significant as expected. The value βT = 0.1 is chosen as the upper limit since the model used for the random variable, X, discussed in Chapter III is only valid for $\beta T \leq 0.3$. The value of βT = 0.01 is chosen as the lower limit for observation since the probability of bit error approaches the case when no laser phase noise is present. The five MFSK cases are next plotted in Figure 11 through 16 for each βT previously observed. The dominance of the laser phase noise on system performance is observed for the lower symbol rates. For example, βT = 0.1, the performance for each of the MFSK cases approaches an

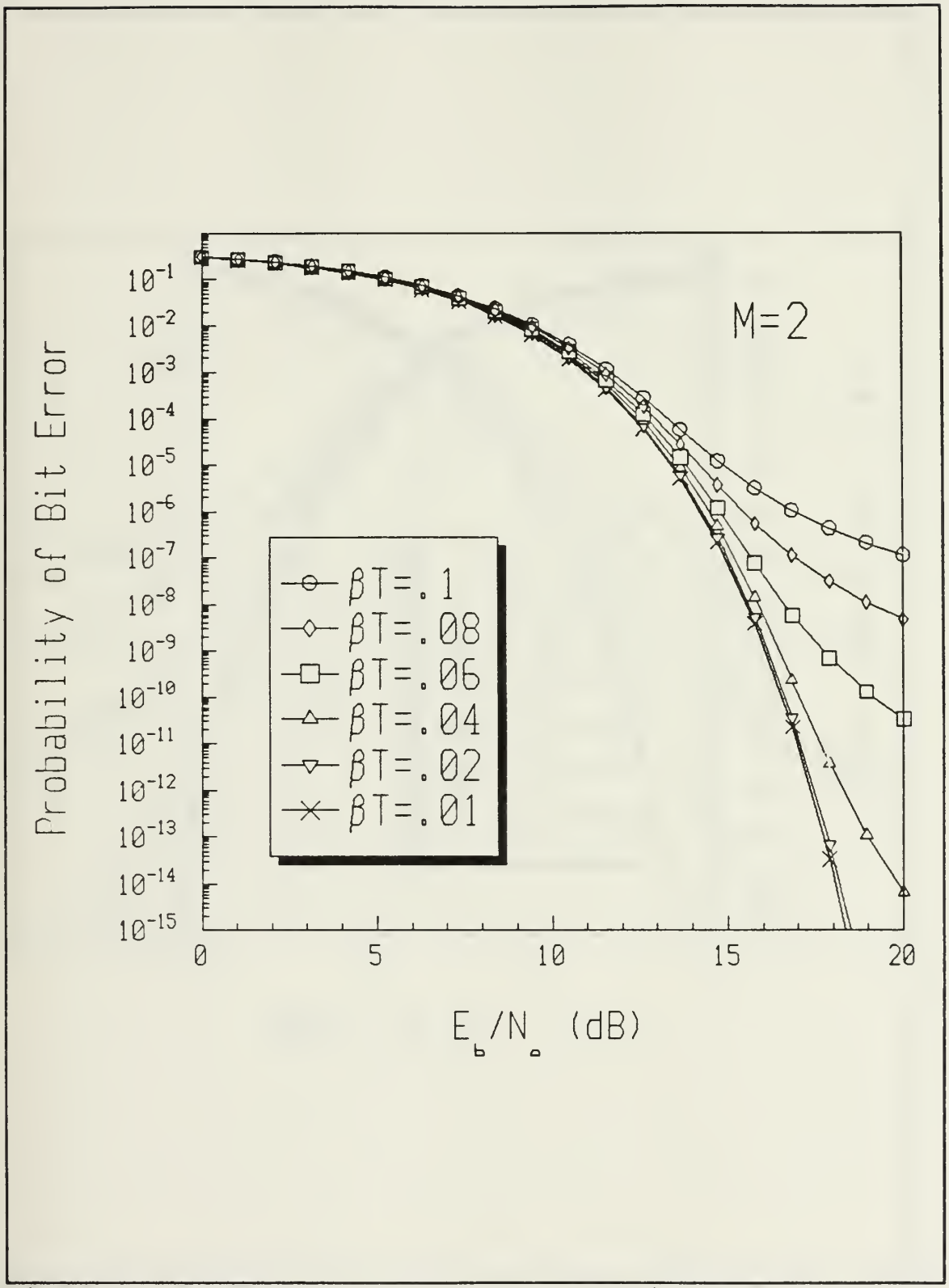

Figure 6 Performance of Coherent Optically Heterodyned MFSK, M = 2

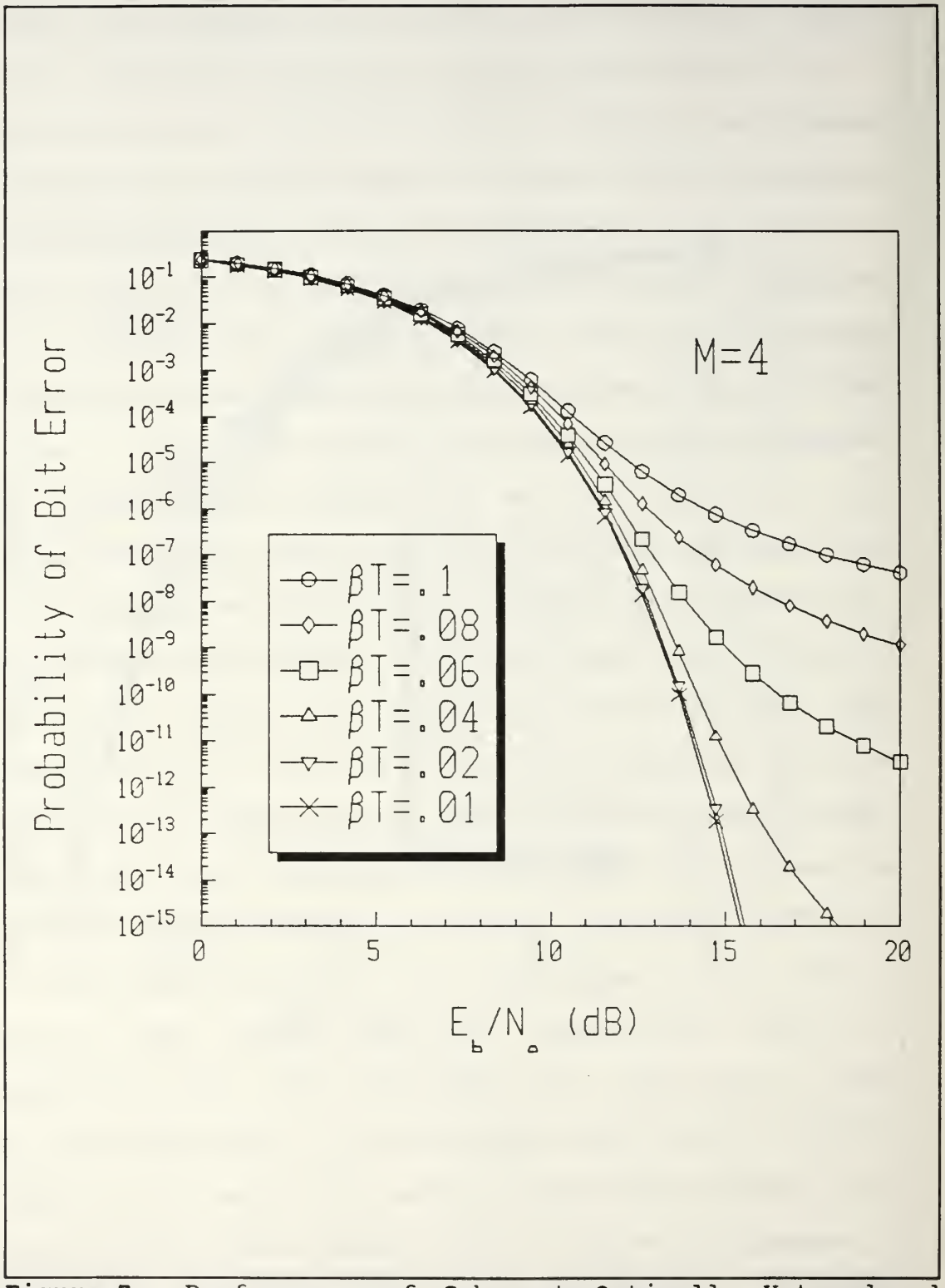

Figure 7 Performance of Coherent Optically Heterodyned MFSK, M = 4

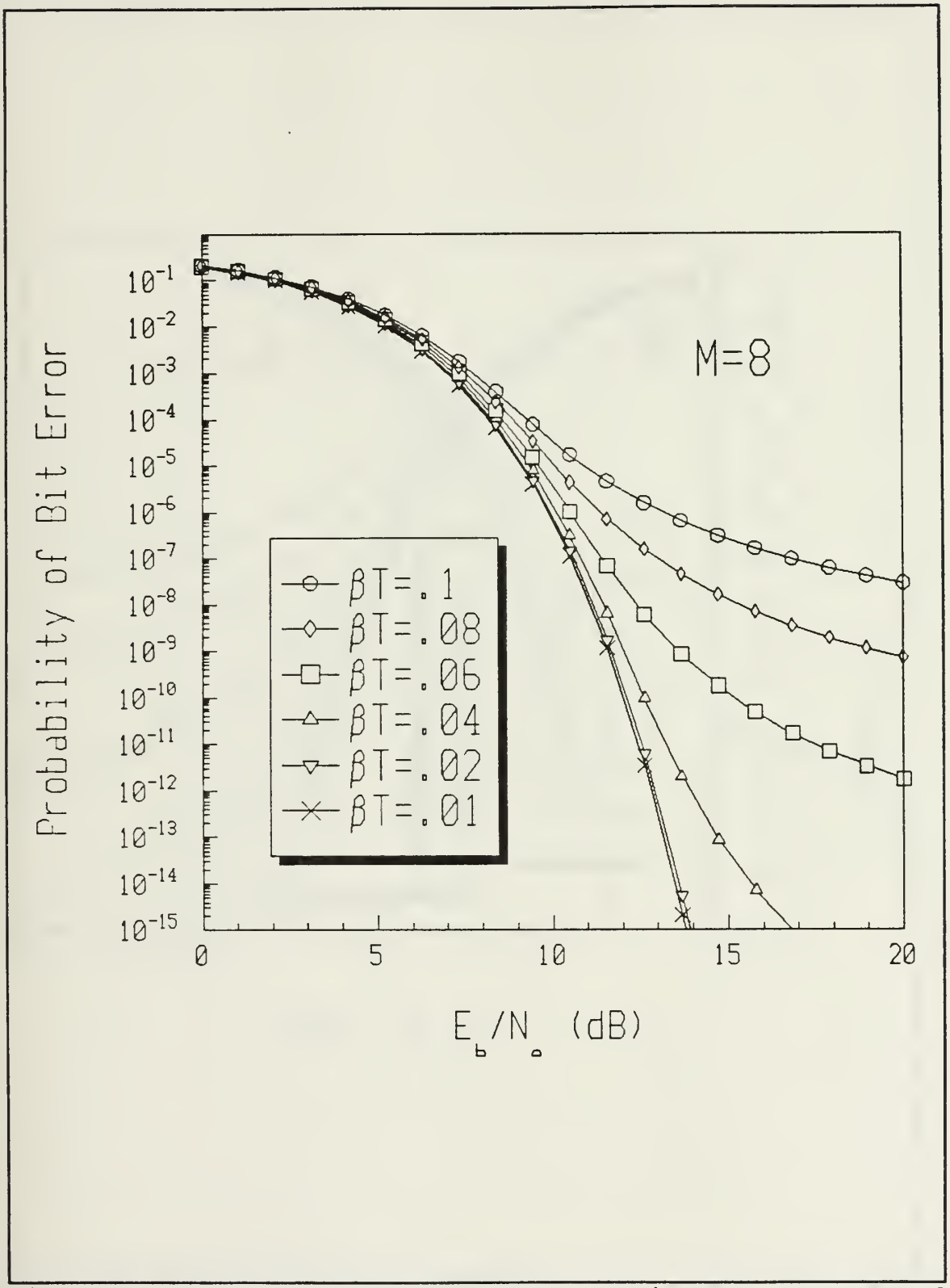

Figure 8 Performance of Coherent Optically Heterodyned MFSK, M = 8

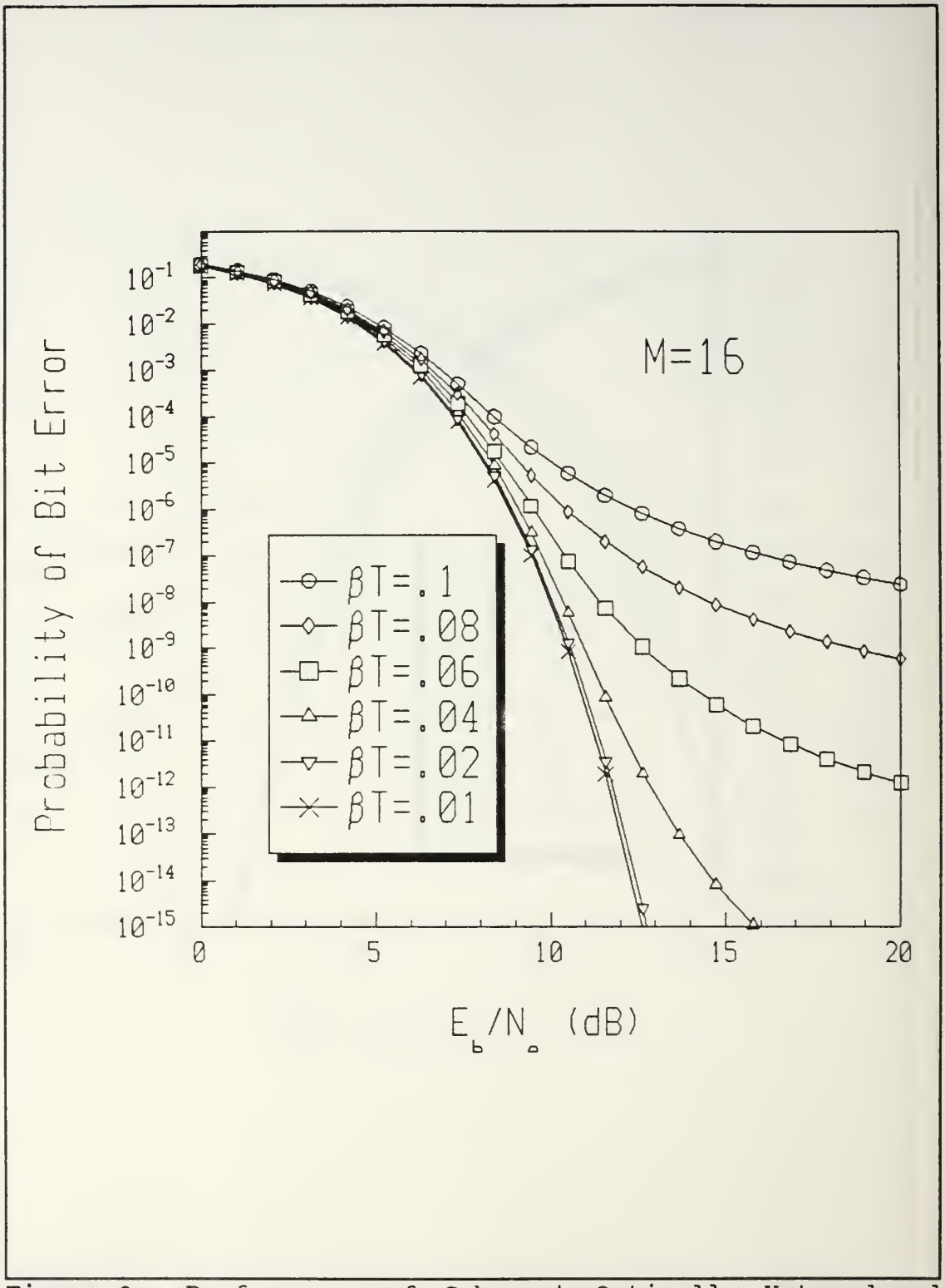

Figure 9 Performance of Coherent Optically Heterodyned MFSK, M = 16

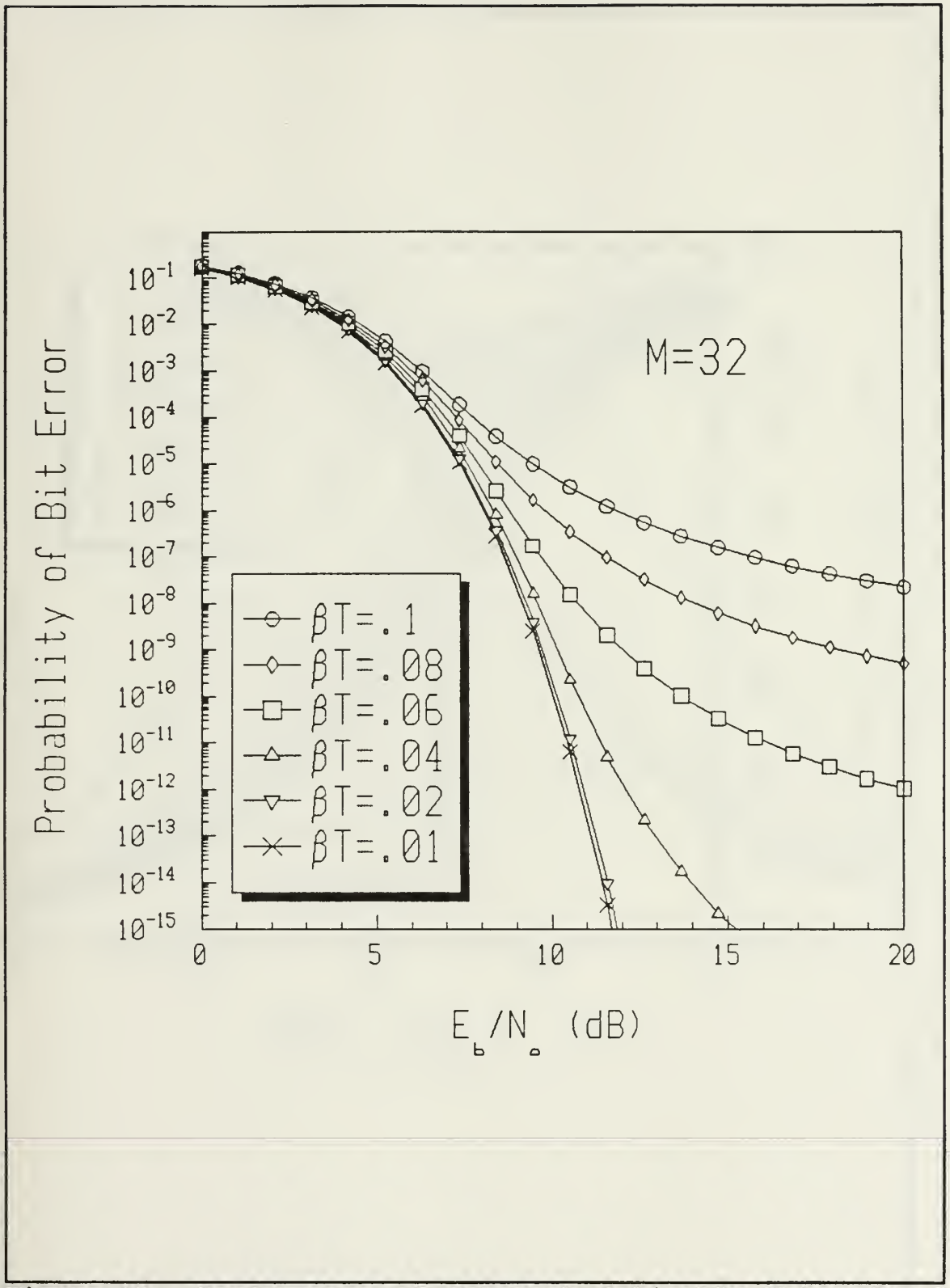

Figure 10 Performance of Coherent Optically Heterodyned MFSK, M = 32

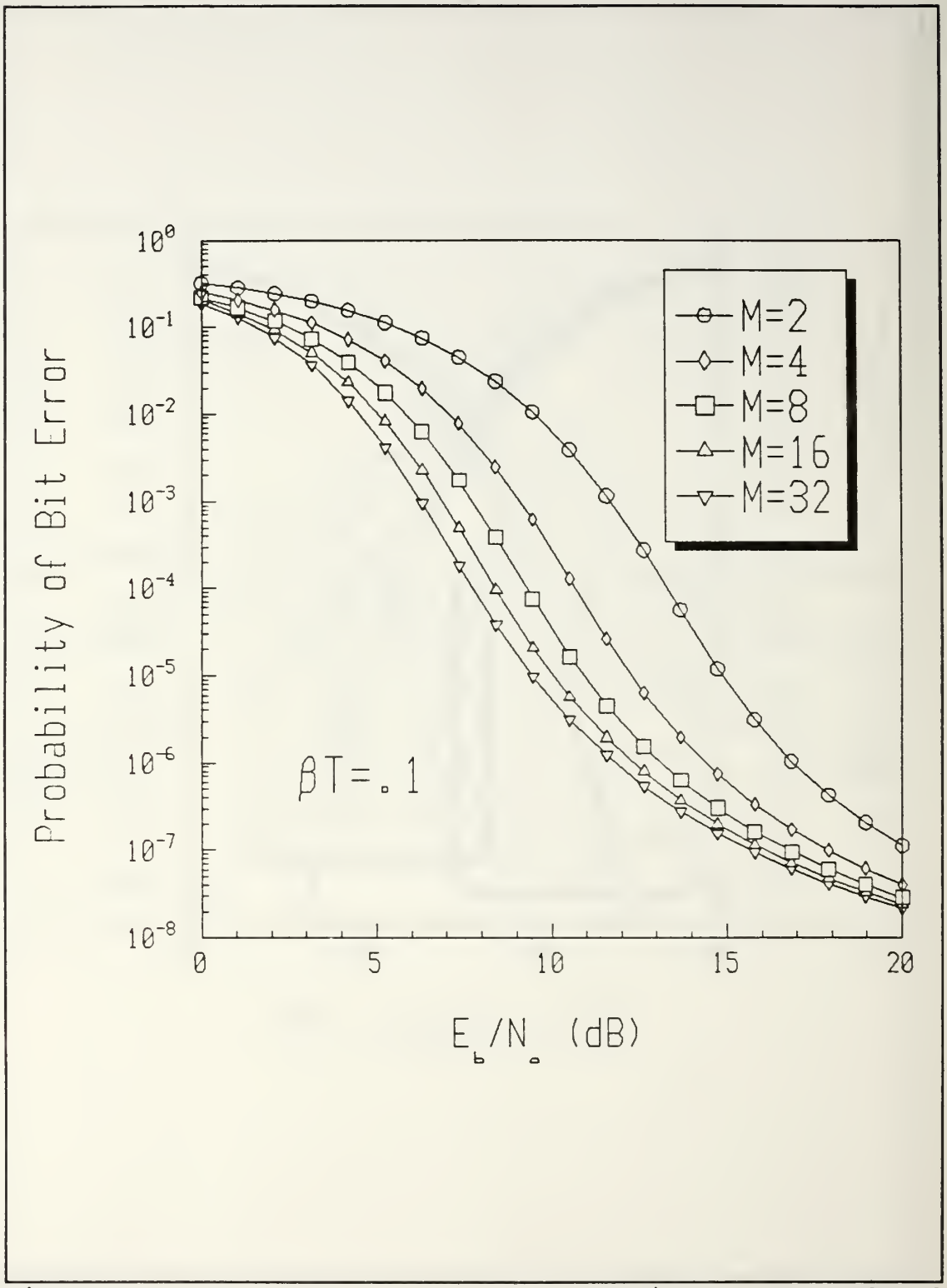

Figure 11 Performance of Coherent Optically Heterodyned MFSK, βT = .1

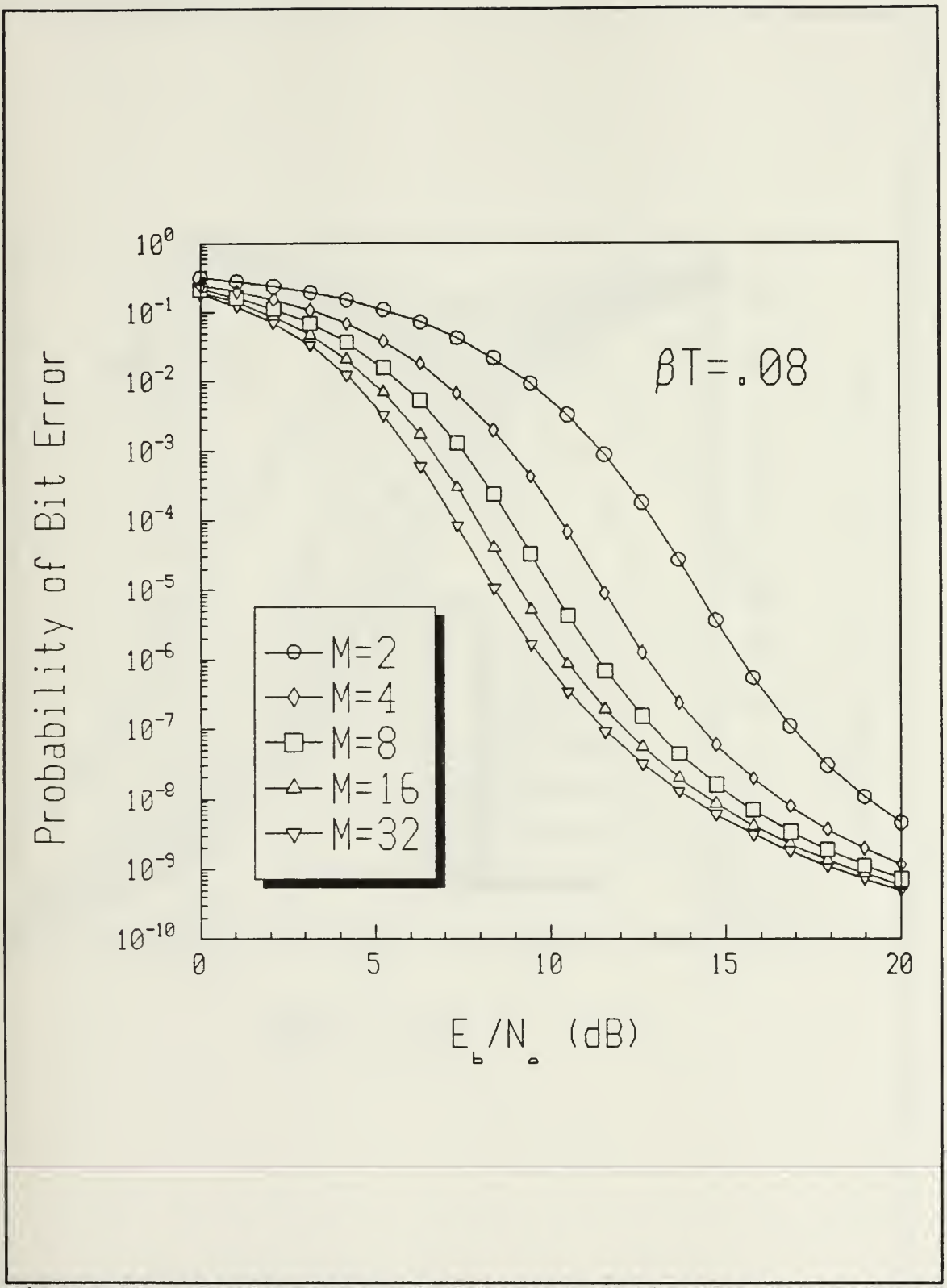

Figure 12 Performance of Coherent Optically Heterodyned MFSK, βT = .08

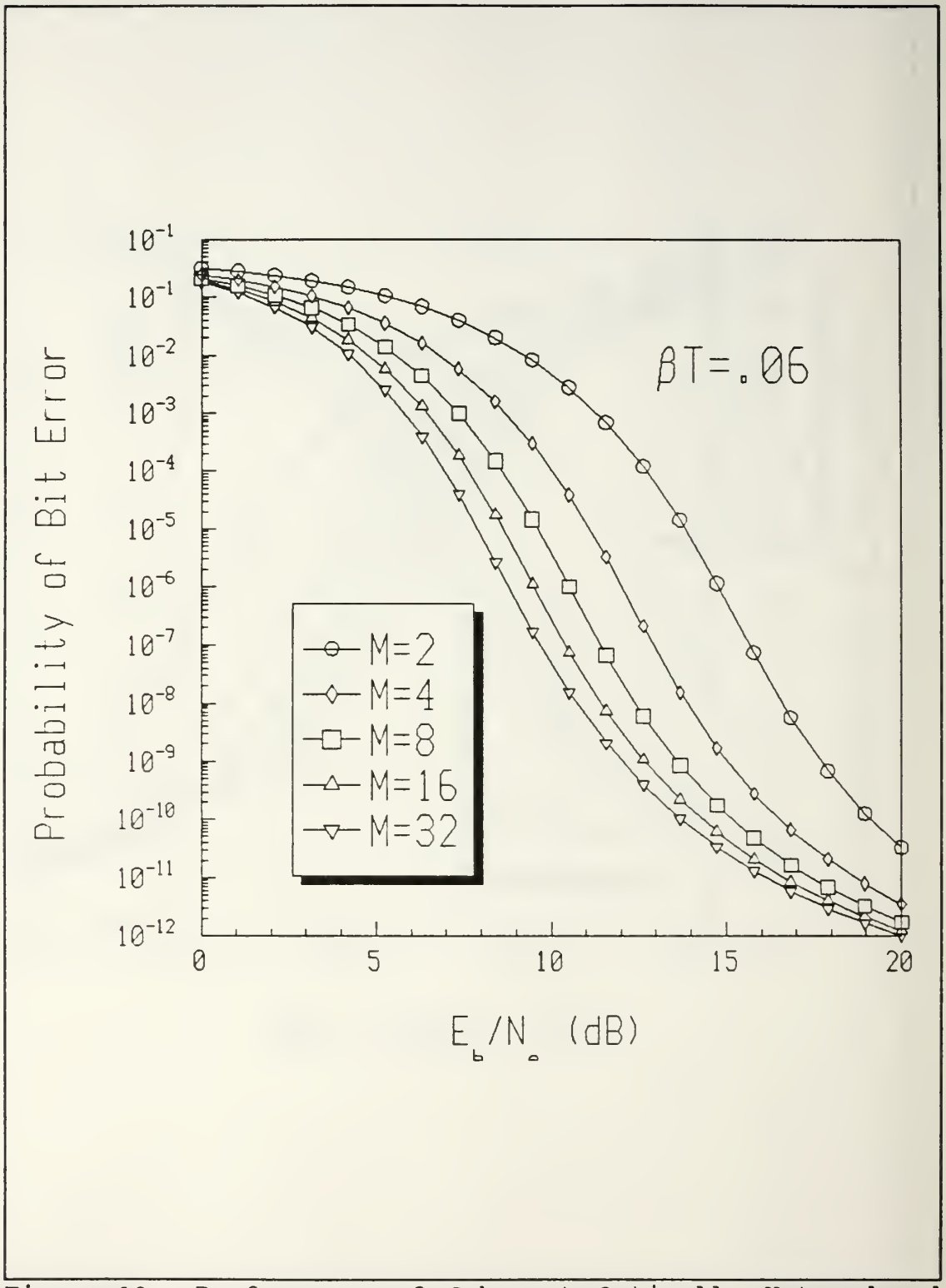

Figure 13 Performance of Coherent Optically Heterodyned MFSK, βT = .06

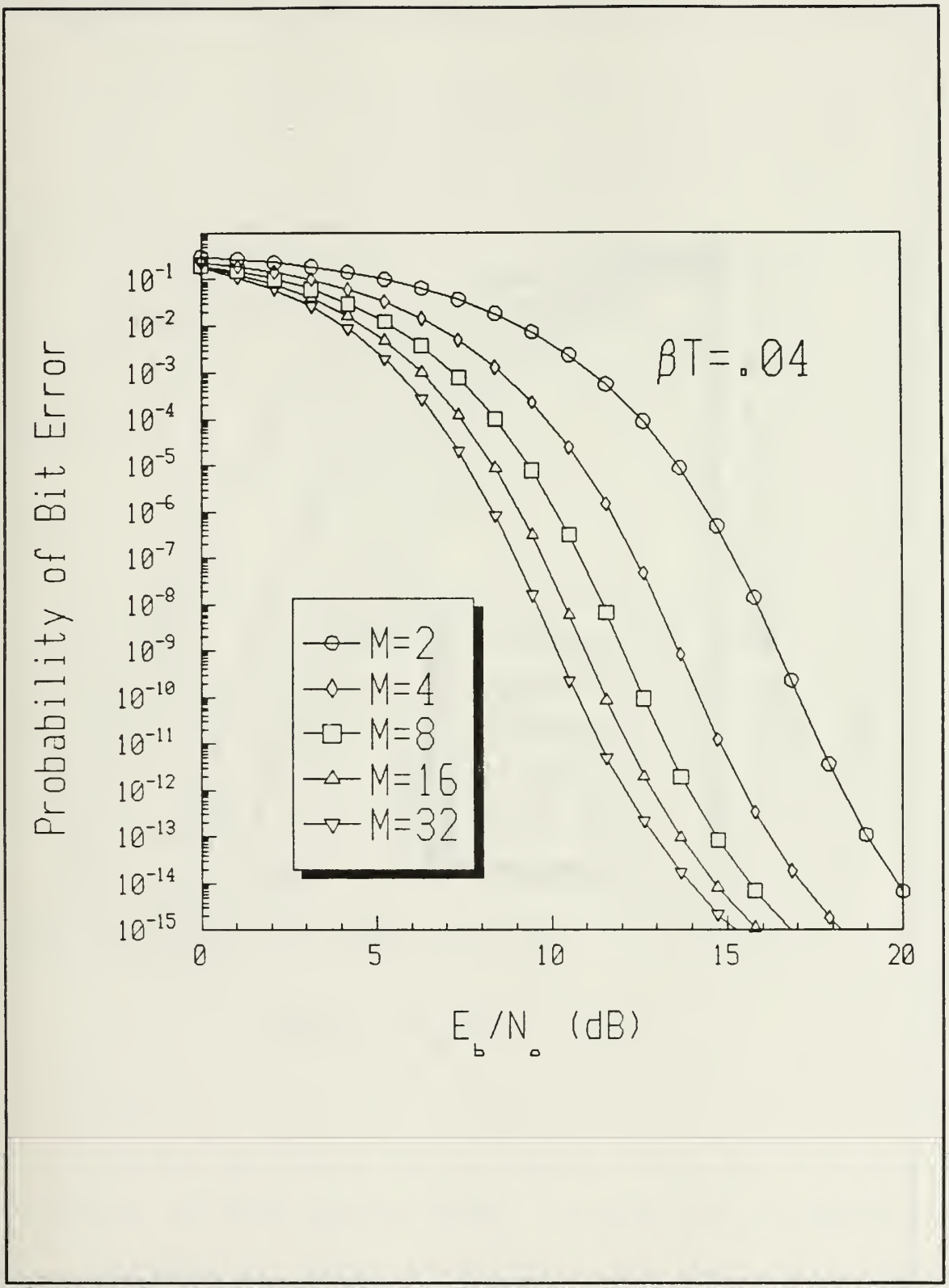

Figure 14 Performance of Coherent Optically Heterodyned MFSK, $\beta T = .04$

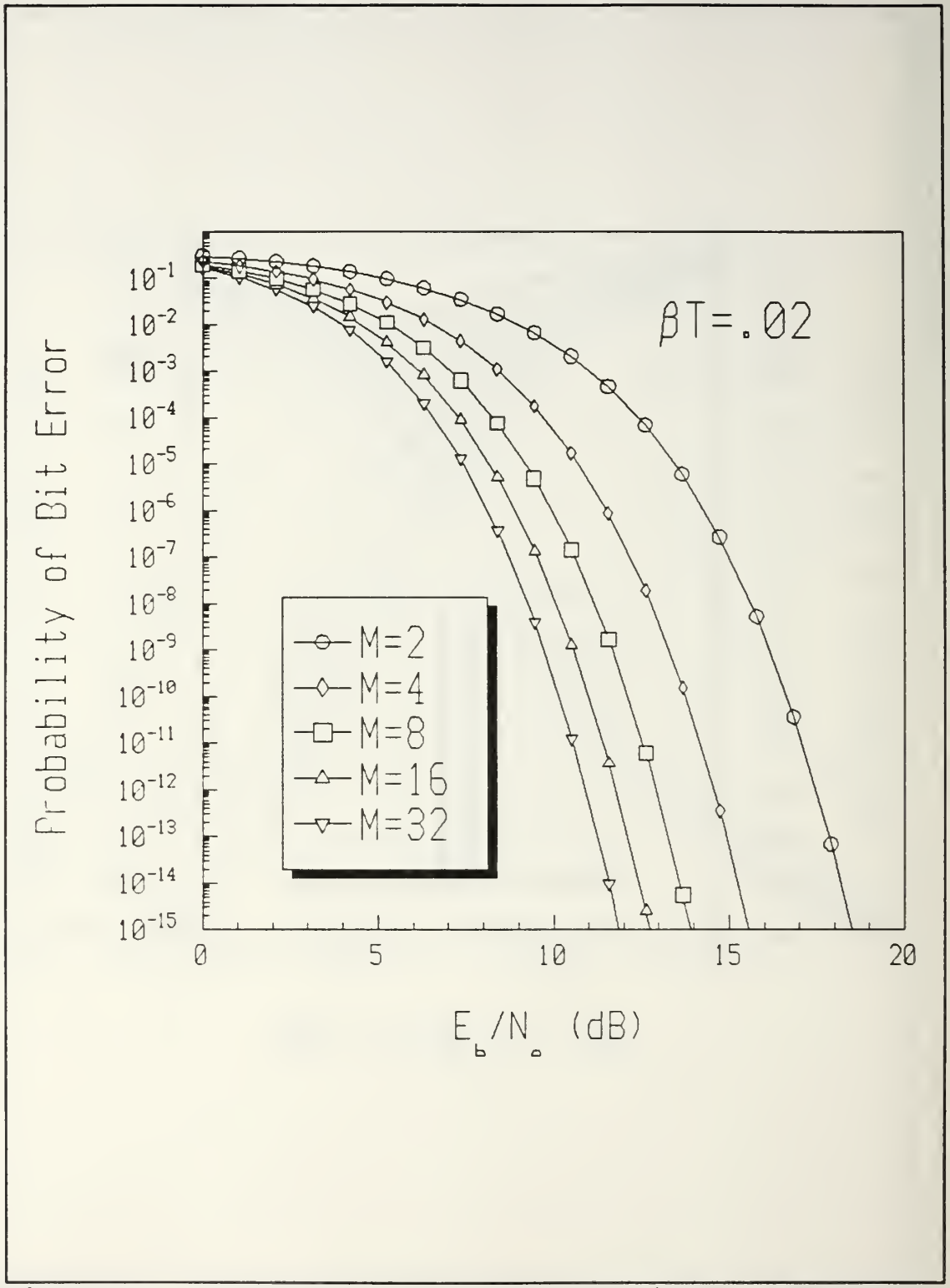

Figure 15 Performance of Coherent Optically Heterodyned MFSK, $\beta T = .02$

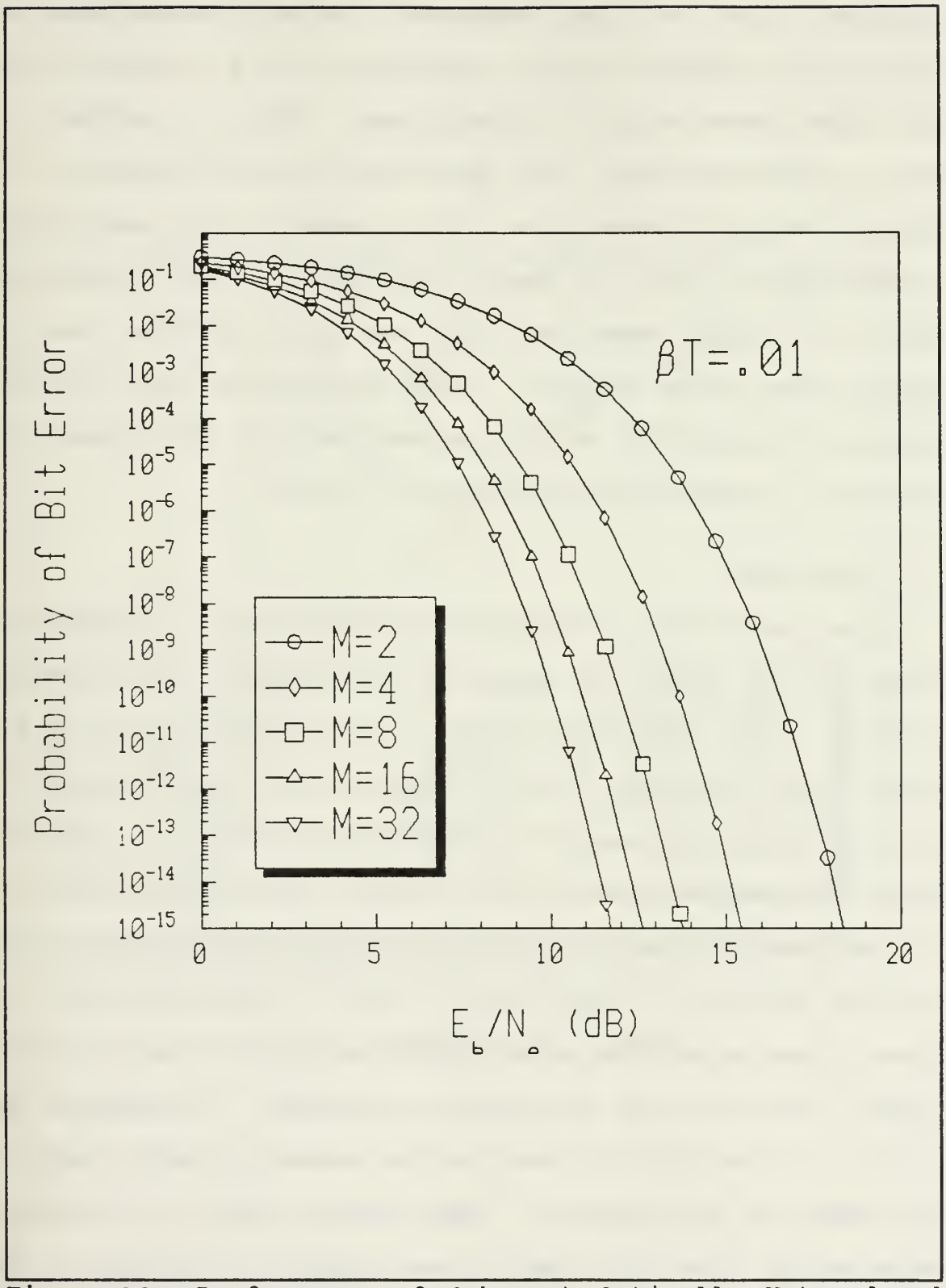

Figure 16 Performance of Coherent Optically Heterodyned MFSK, $\beta T = .01$

asymptotic limit as E_b/N_0 increases. The performance does not continue to improve as E_b/N_0 increases or as M increases when the laser phase noise is significant. This is contrary to what is observed when laser phase noise is not present. As another example, when $\beta T = 0.04$, a symbol rate twenty-five times greater than the laser linewidth, the performance of each of the MFSK cases is within one dB of the case when no laser phase noise exists. These conclusions apply to the range of probability of bit errors that are of concern for practical communication systems, 10^{-9} to 10^{-6}.

B. MFSK-CDMA

The probability of bit error for MFSK-CDMA is expressed in terms of the number of users and the symbol rate linewidth product. The MFSK-CDMA analysis is performed by using the noise term, Equation (50), in Equation (43). In Figures 17 through 21 the performance is observed for $\beta T = 0.1$, when the symbol rate is ten times the linewidth, for various values of M. Few users can be added to the system since the performance is poor even for a single user. This is expected since the laser phase noise dominates system performance for the lower symbol rates as was previously discussed. Increasing the value of M has little impact on the number of users that can be added to the system. Once again, this is consistent considering that the laser phase noise is dominant. The opposite is observed in Figures 22 through 26. For this

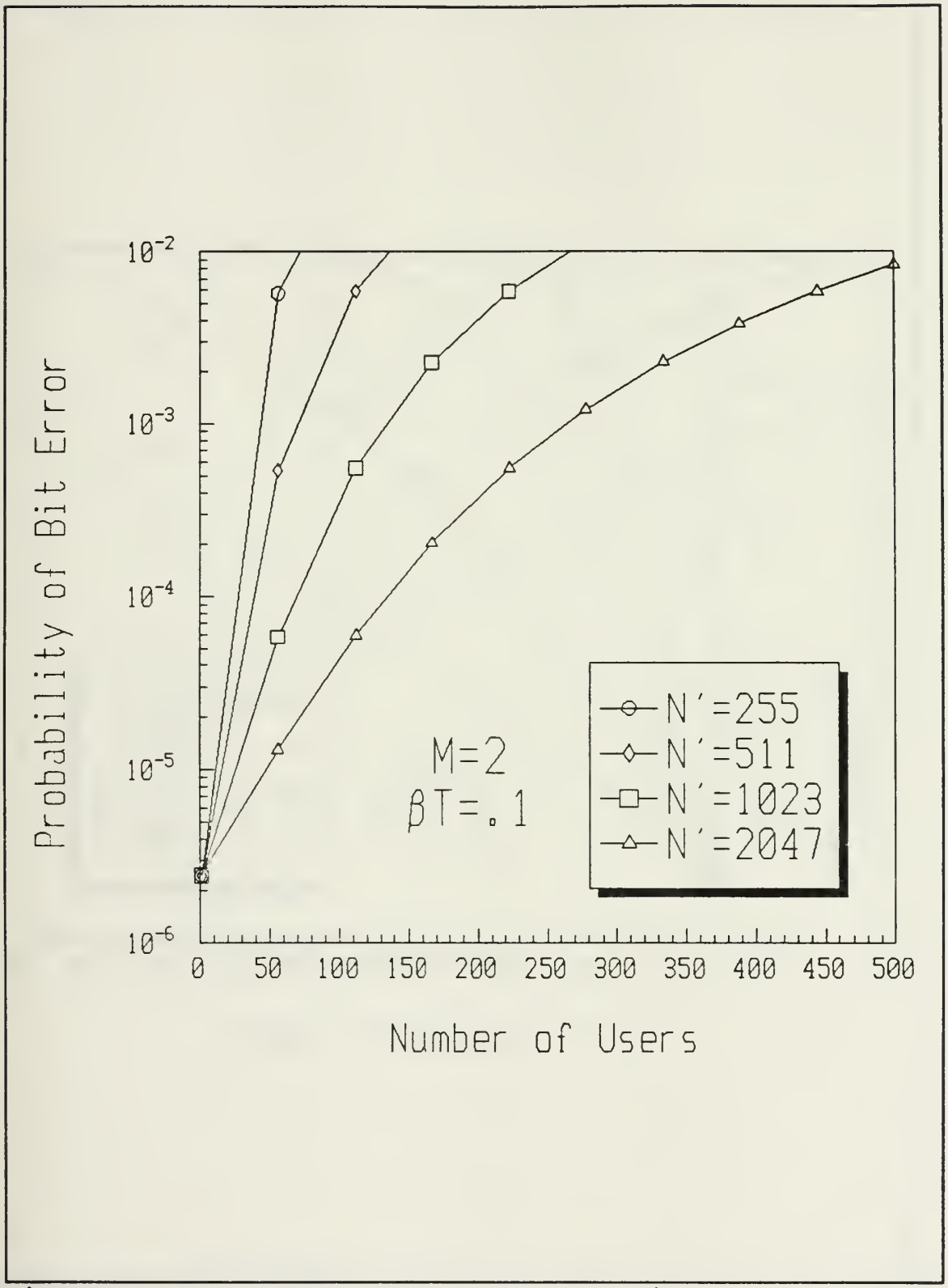

Figure 17 Performance of Coherent Optically Heterodyned MFSK-CDMA, M=2 and βT = .1

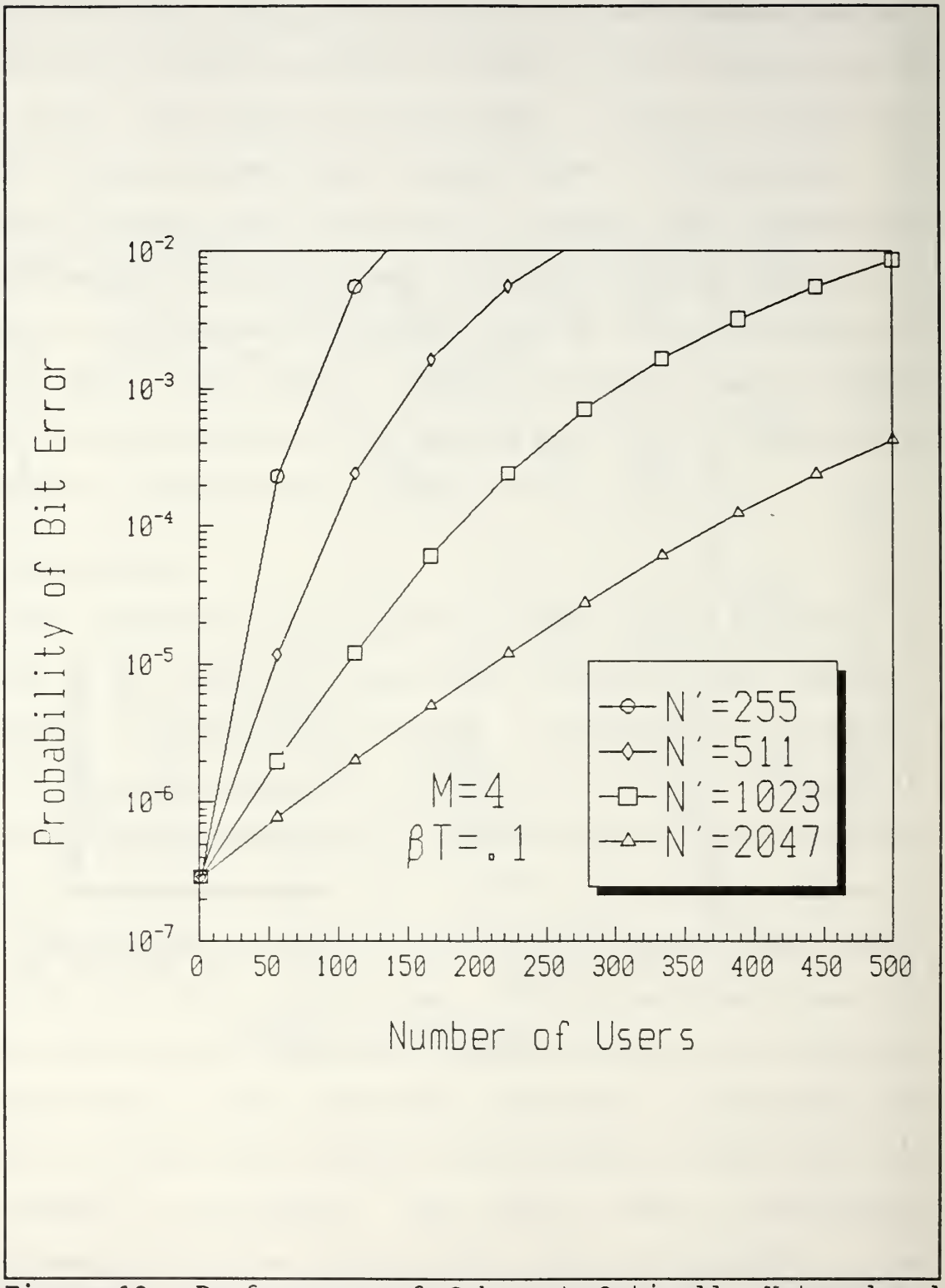

Figure 18 Performance of Coherent Optically Heterodyned MFSK-CDMA, M=4 and βT = .1

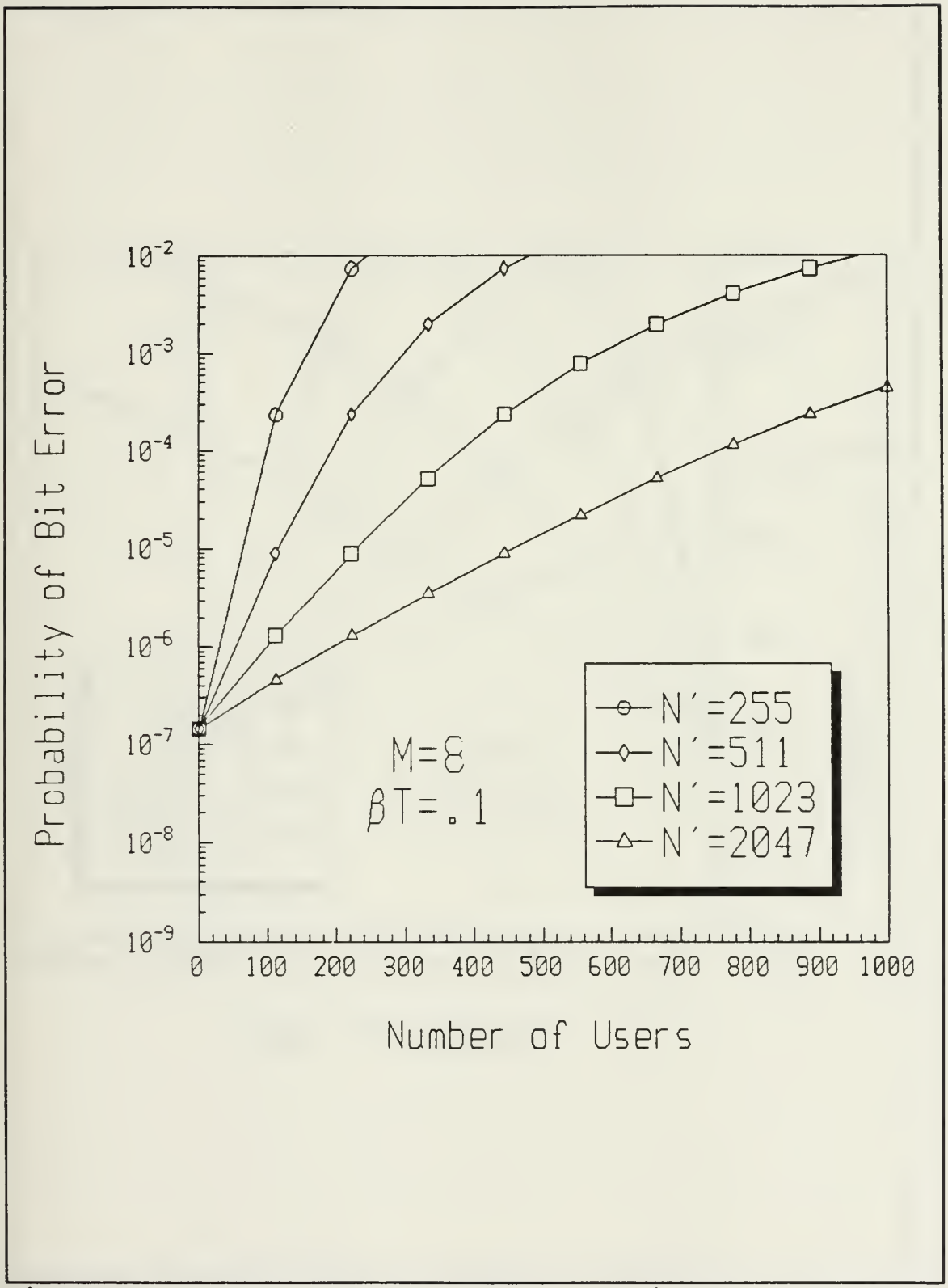

Figure 19 Performance of Coherent Optically Heterodyned MFSK-CDMA, M = 8 and βT = .1

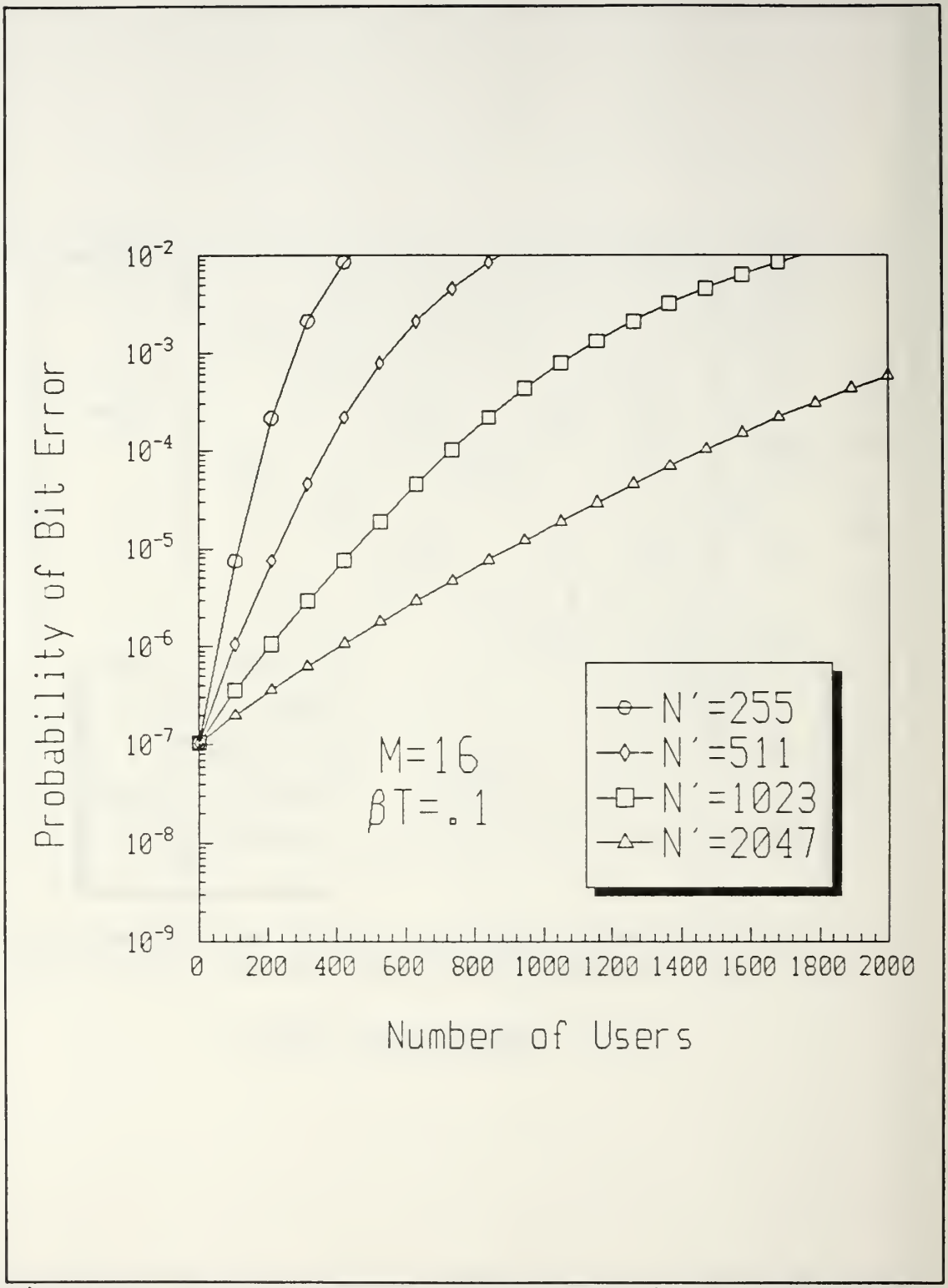

Figure 20 Performance of Coherent Optically Heterodyned MFSK-CDMA, M = 16 and βT = .1

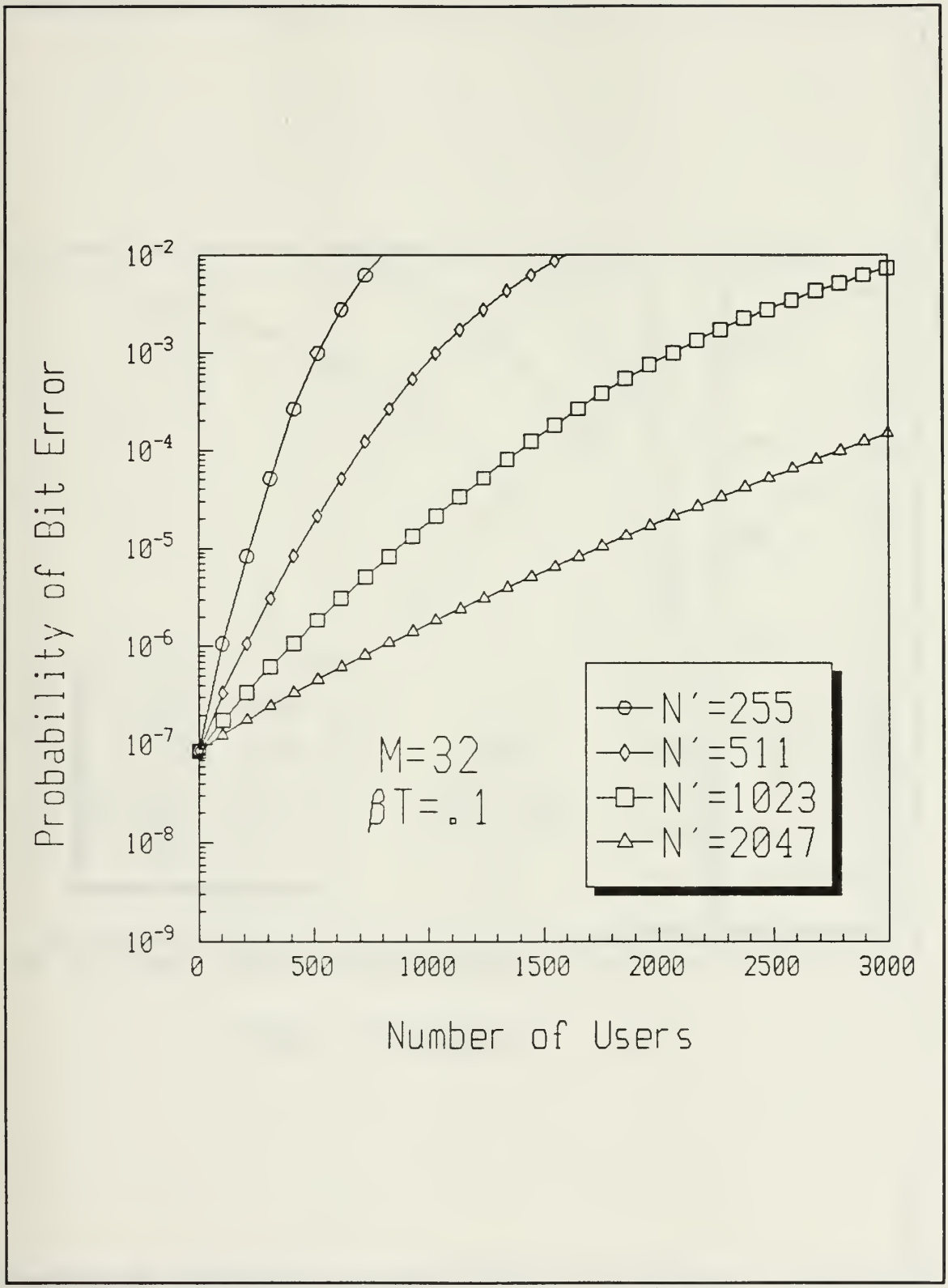

Figure 21 Performance of Coherent Optically Heterodyned MFSK-CDMA, M = 32 and βT = .1

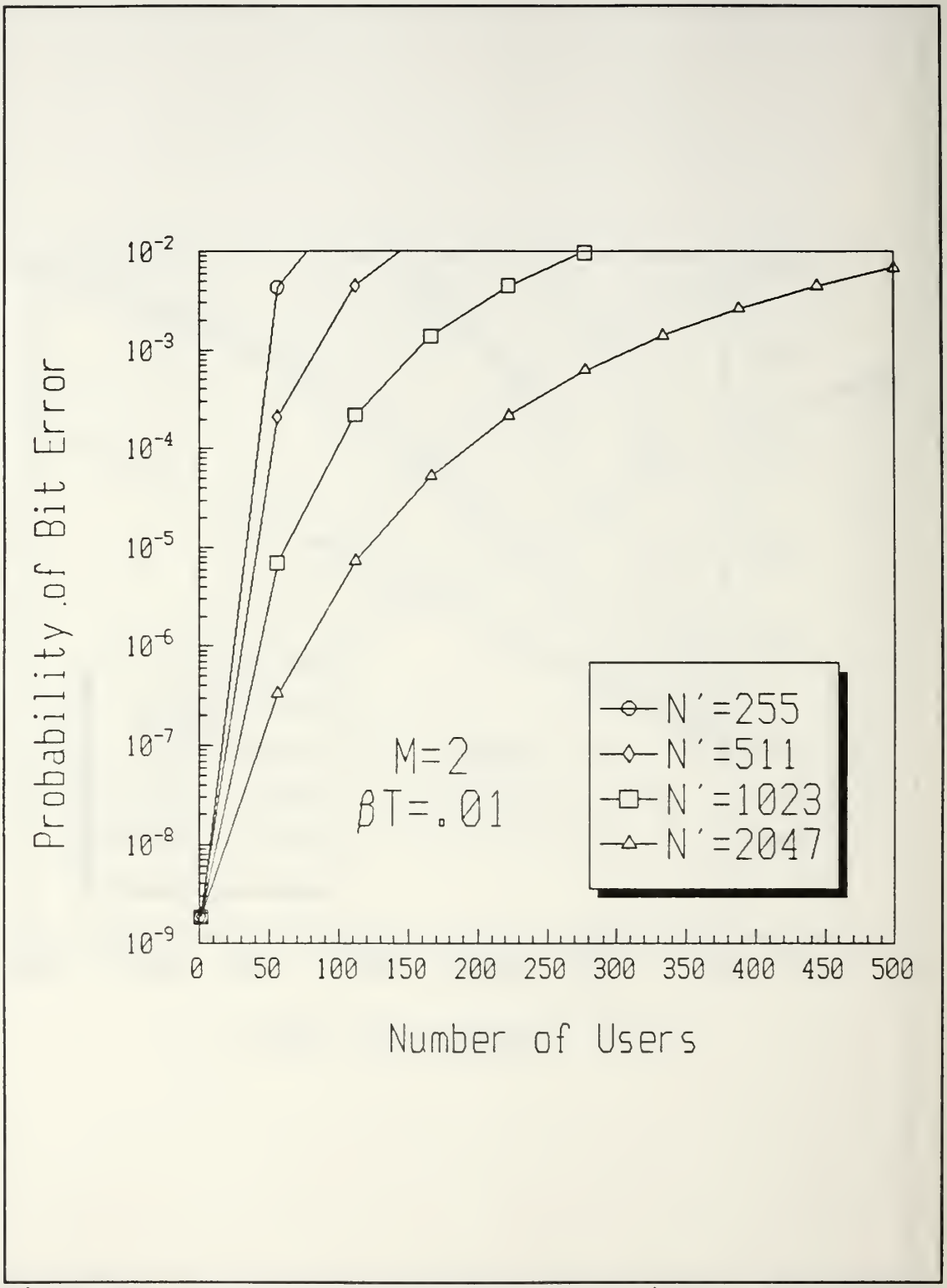

Figure 22 Performance of Coherent Optically Heterodyned MFSK-CDMA, M = 2 and βT = .01

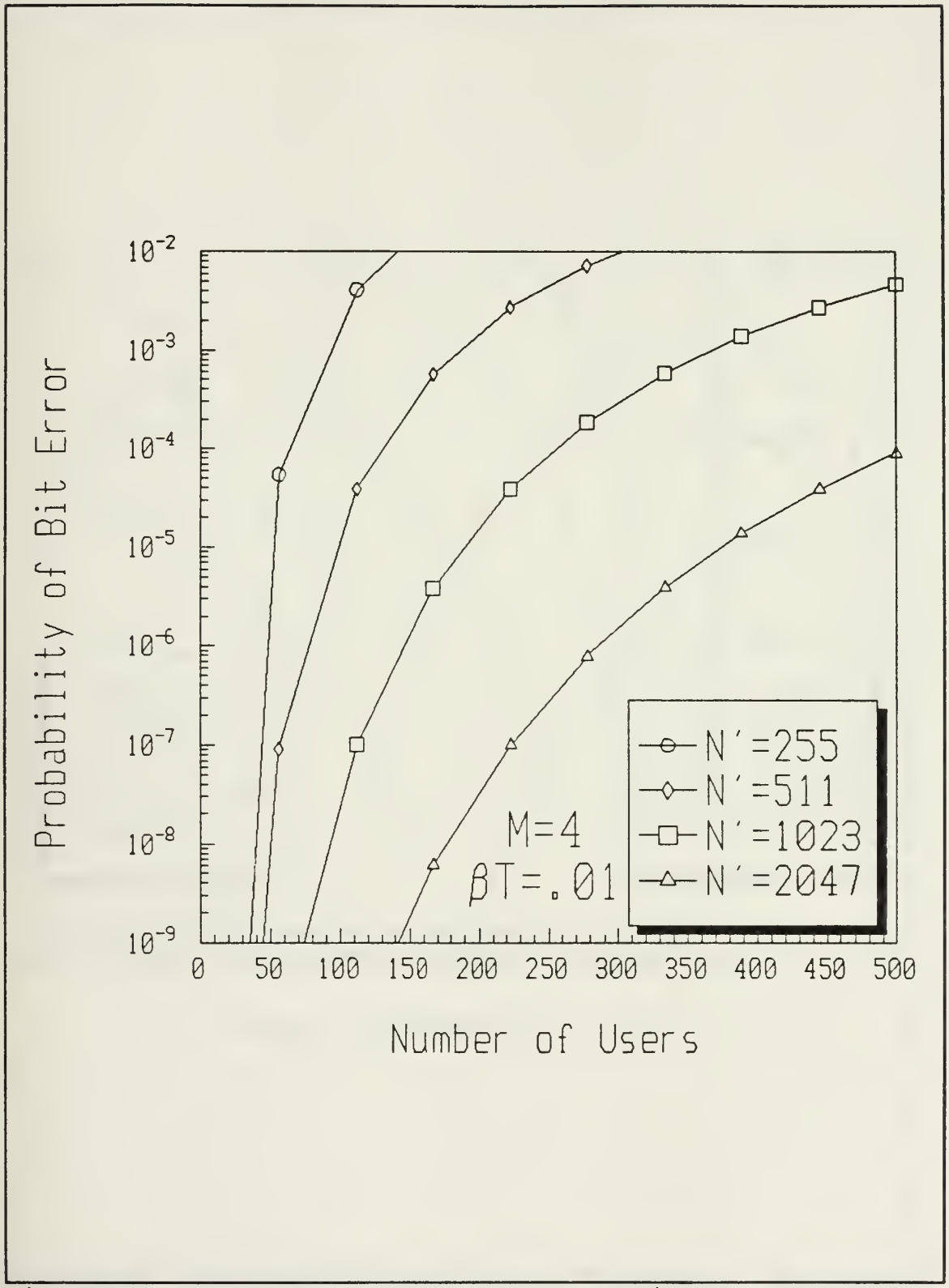

Figure 23 Performance of Coherent Optically Heterodyned MFSK-CDMA, M = 4 and βT = .01

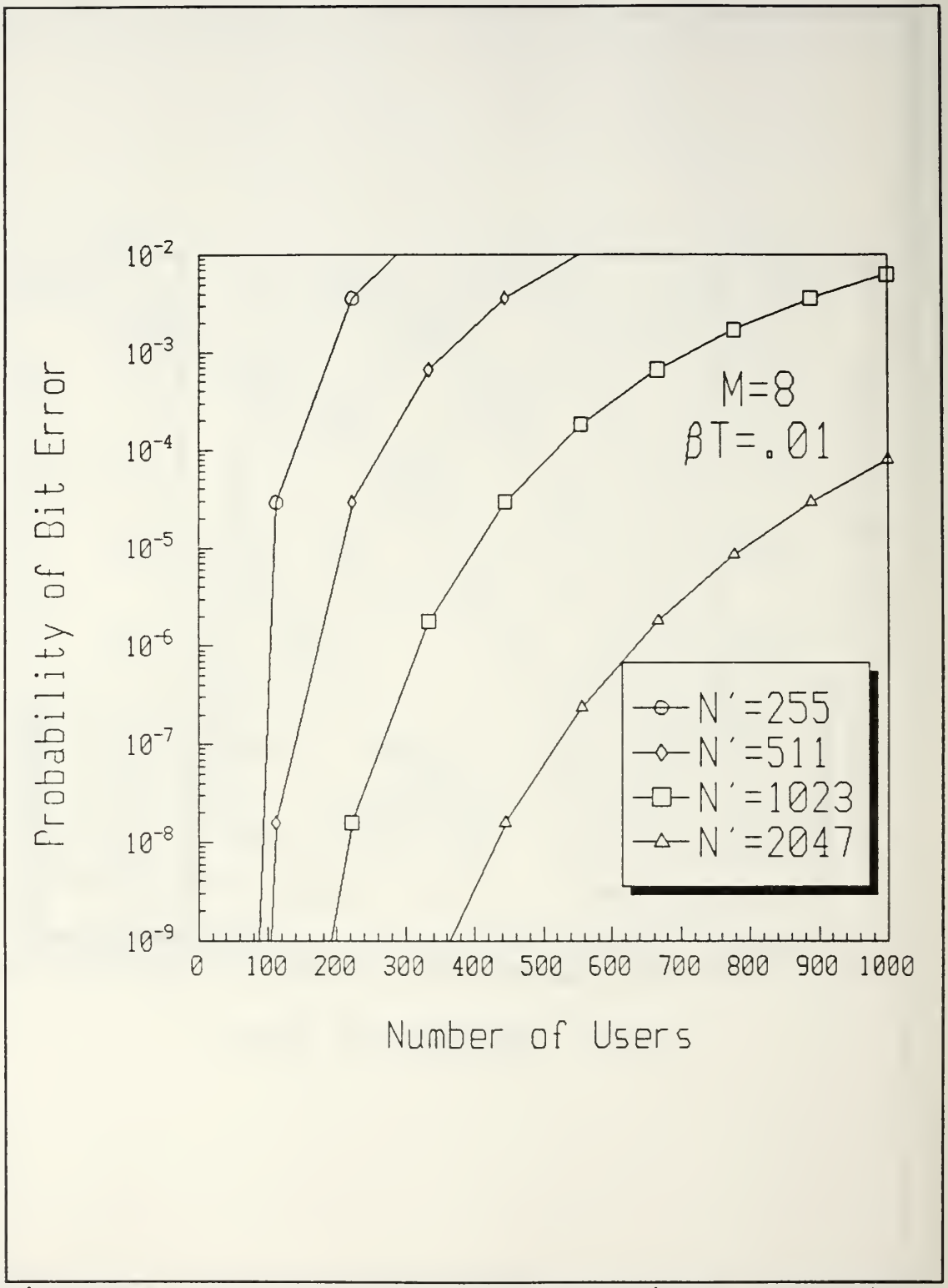

Figure 24 Performance of Coherent Optically Heterodyned MFSK-CDMA, M = 8 and βT = .01

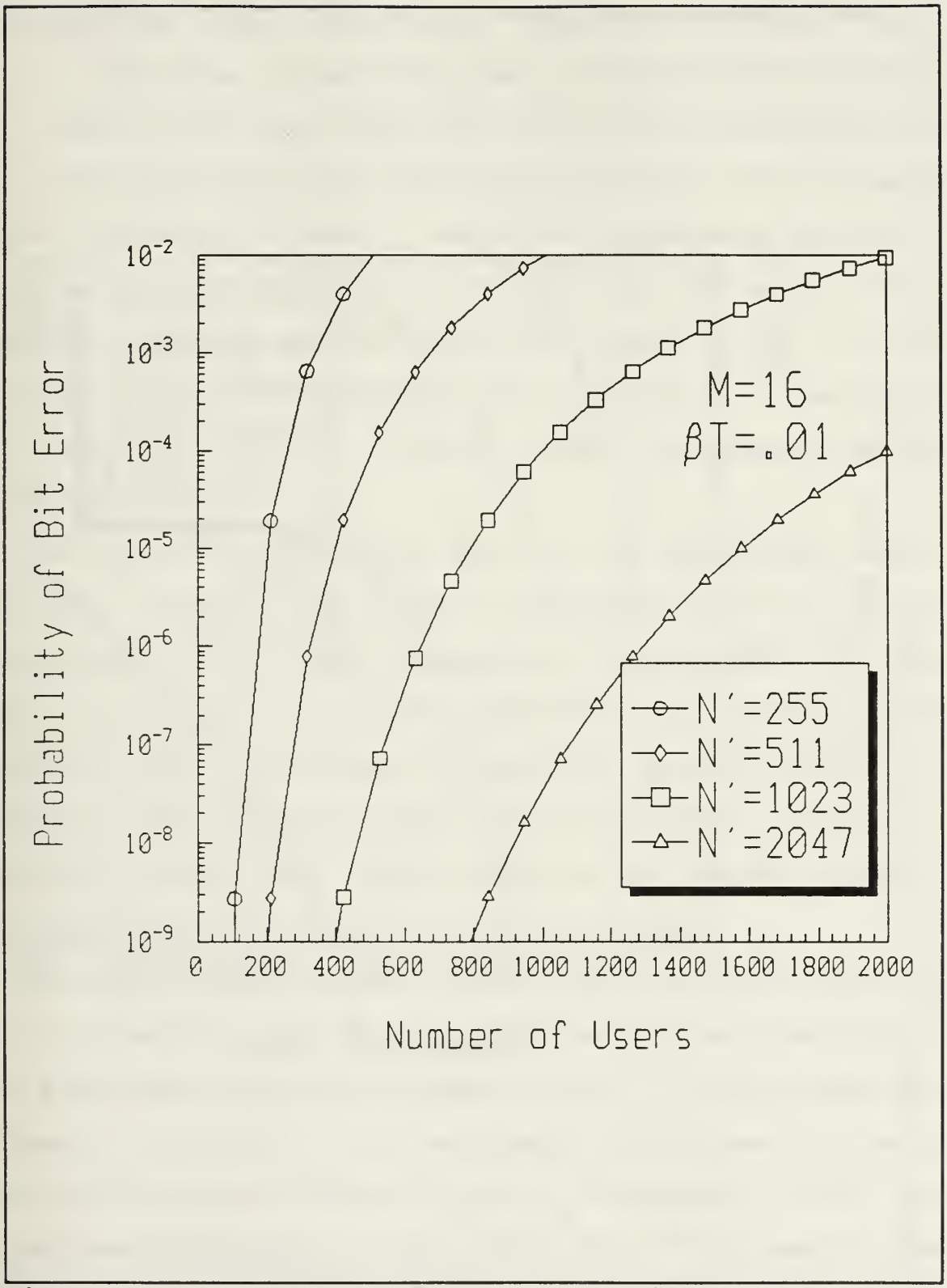

Figure 25 Performance of Coherent Optically Heterodyned MFSK-CDMA, M = 16 and βT = .01

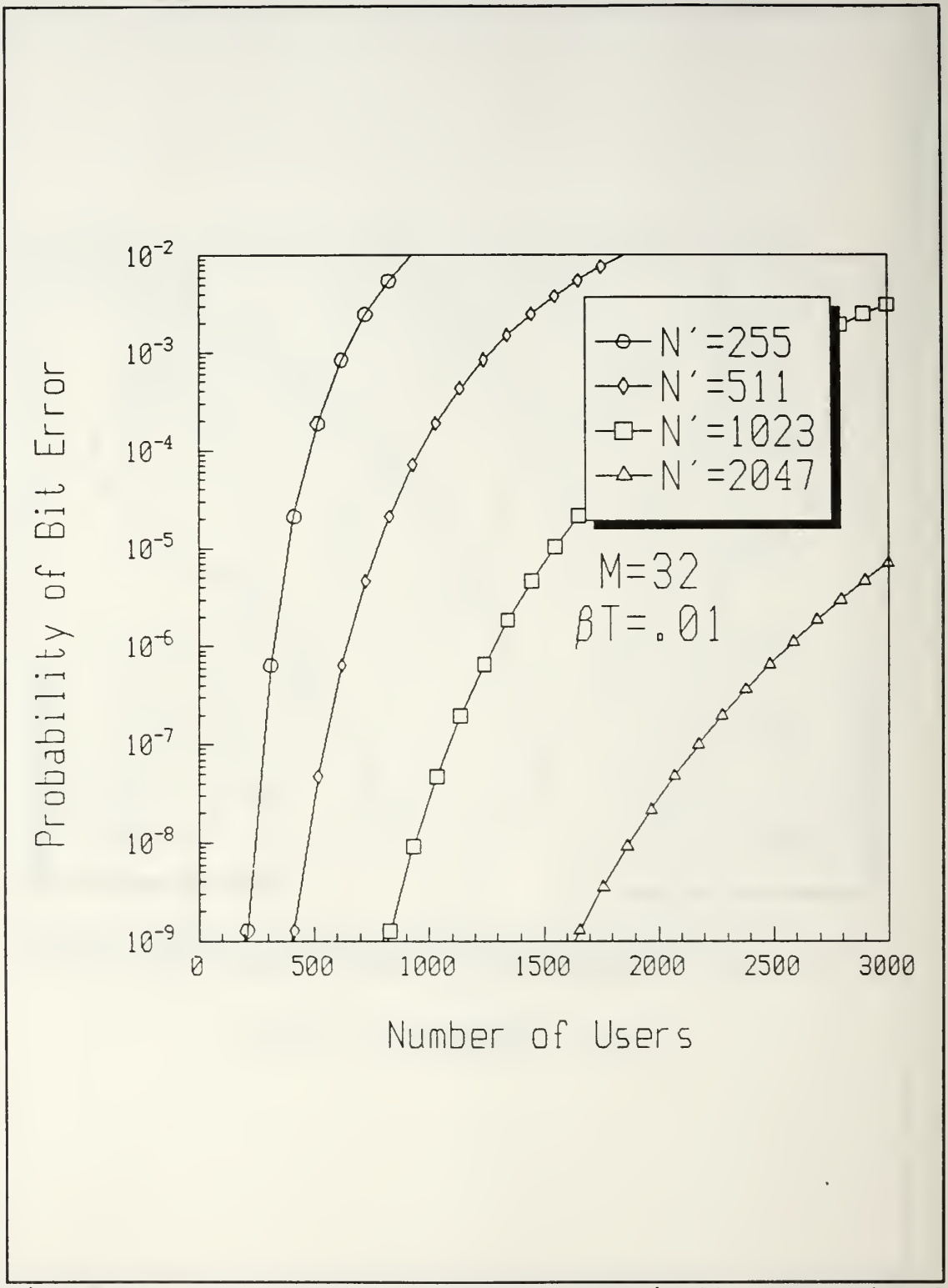

Figure 26 Performance of Coherent Optically Heterodyned MFSK-CDMA, M = 32 and βT = .01

analysis the symbol rate is 100 times the linewidth, βT = 0.01. The number of users obviously increases from the βT = 0.1 case for the same value of M and a given probability of bit error since the laser phase noise no longer has an impact on the system performance. The system performance when βT = 0.01 is degraded only by the addition of more users to the system. Since the maximum average bit energy is set to 16 dB for all of the MFSK analyses, then the SNR is larger as M increases resulting in a better system performance which allows more users.

In either the βT = 0.1 or the βT = 0.01 cases, the number of users increases for longer codelengths before a given minimum performance level is reached. This is true for CDMA systems in general. As the codelength is increased, the amount of noise that a single interfering user contributes is smaller if the amount of signal power received is normalized. Therefore, more users can be added to the system before a specific minimum performance level is attained.

For the single user MFSK, the system performance when βT = 0.04 is degraded only slightly because of laser phase noise. The MFSK-CDMA system performance for βT = 0.04 is shown in Figures 27 through 31. As an example, the number of users that can access the system for M = 4, codelength = 1023, and a maximum probability of bit error of 10^{-6} increases from approximately 40 users for βT = 0.1 to 130 users for βT = 0.04. This improvement requires only a symbol rate of twenty-

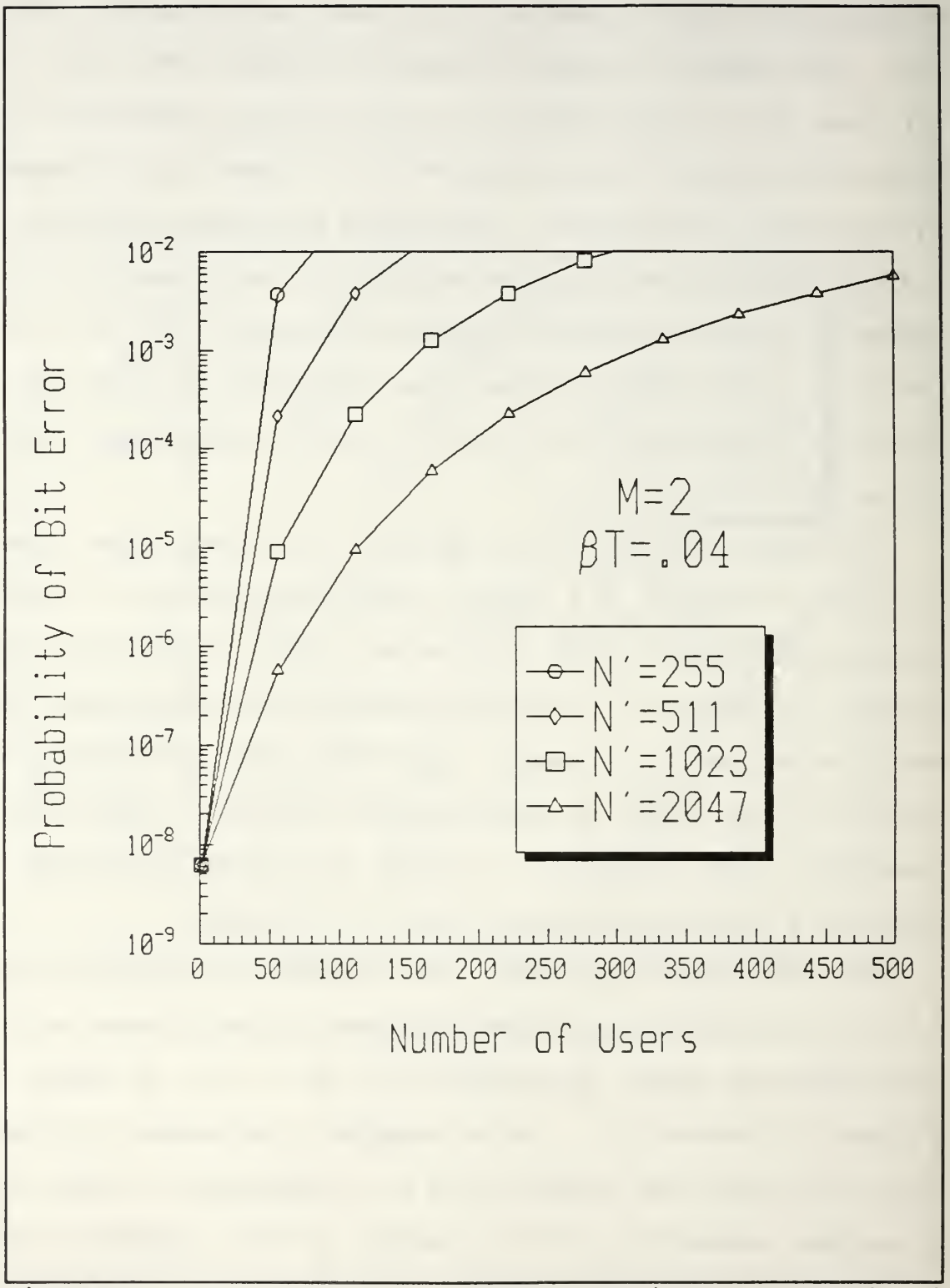

Figure 27 Performance of Coherent Optically Heterodyned MFSK-CDMA, M = 2 and βT = .04

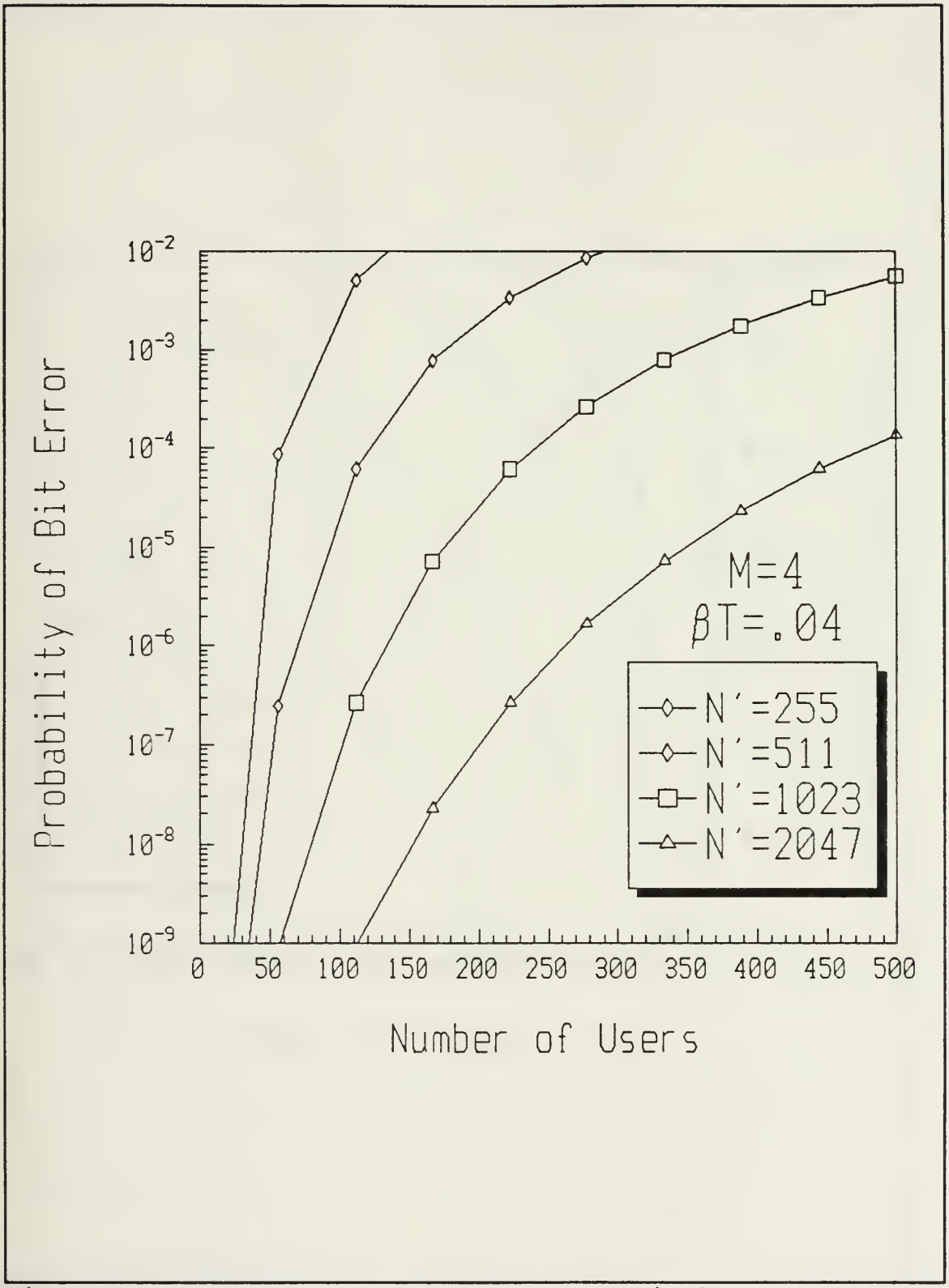

Figure 28 Performance of Coherent Optically Heterodyned MFSK-CDMA, M = 4 and βT = .04

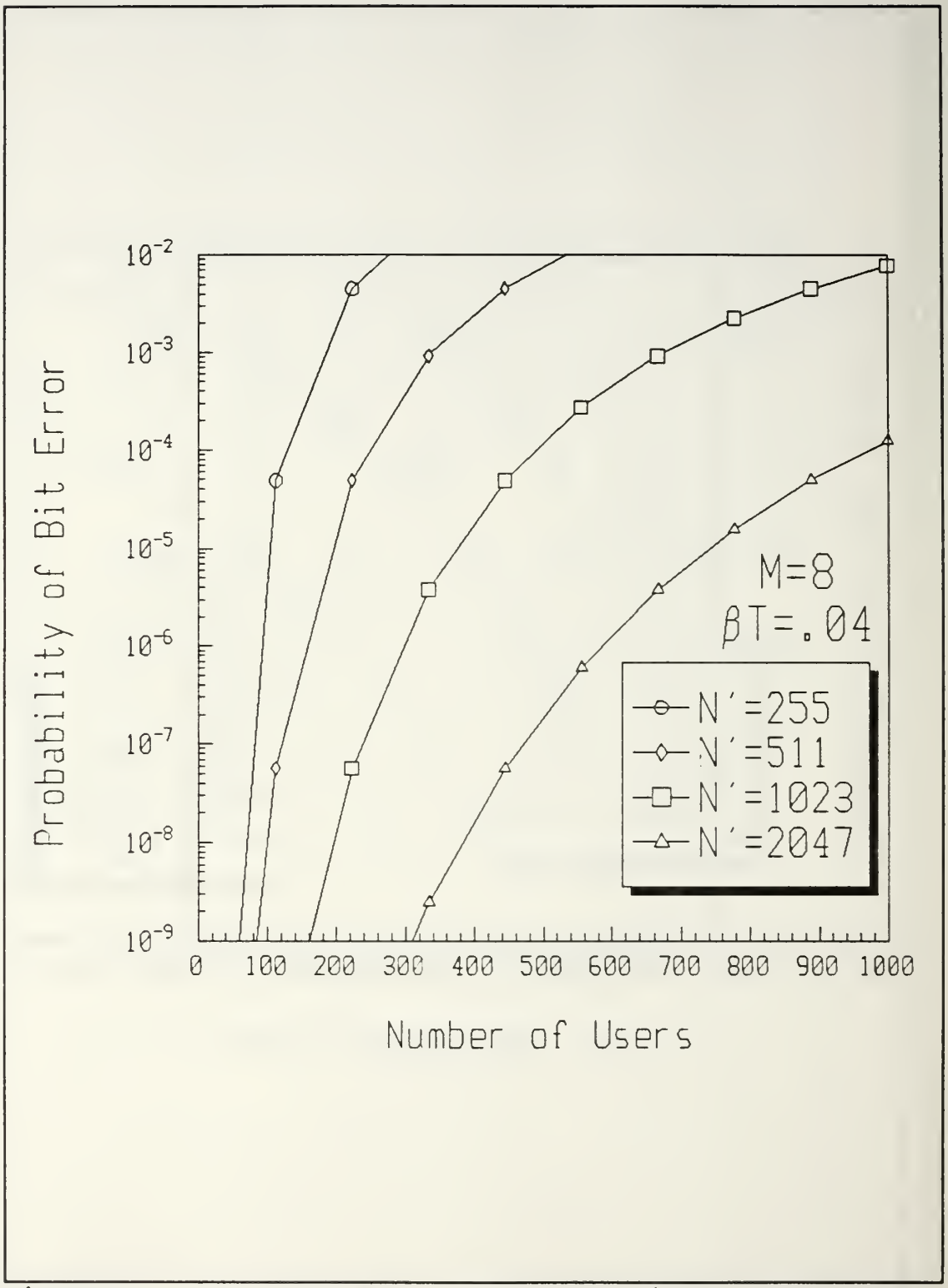

Figure 29 Performance of Coherent Optically Heterodyned MFSK-CDMA, M = 8 and βT = .04

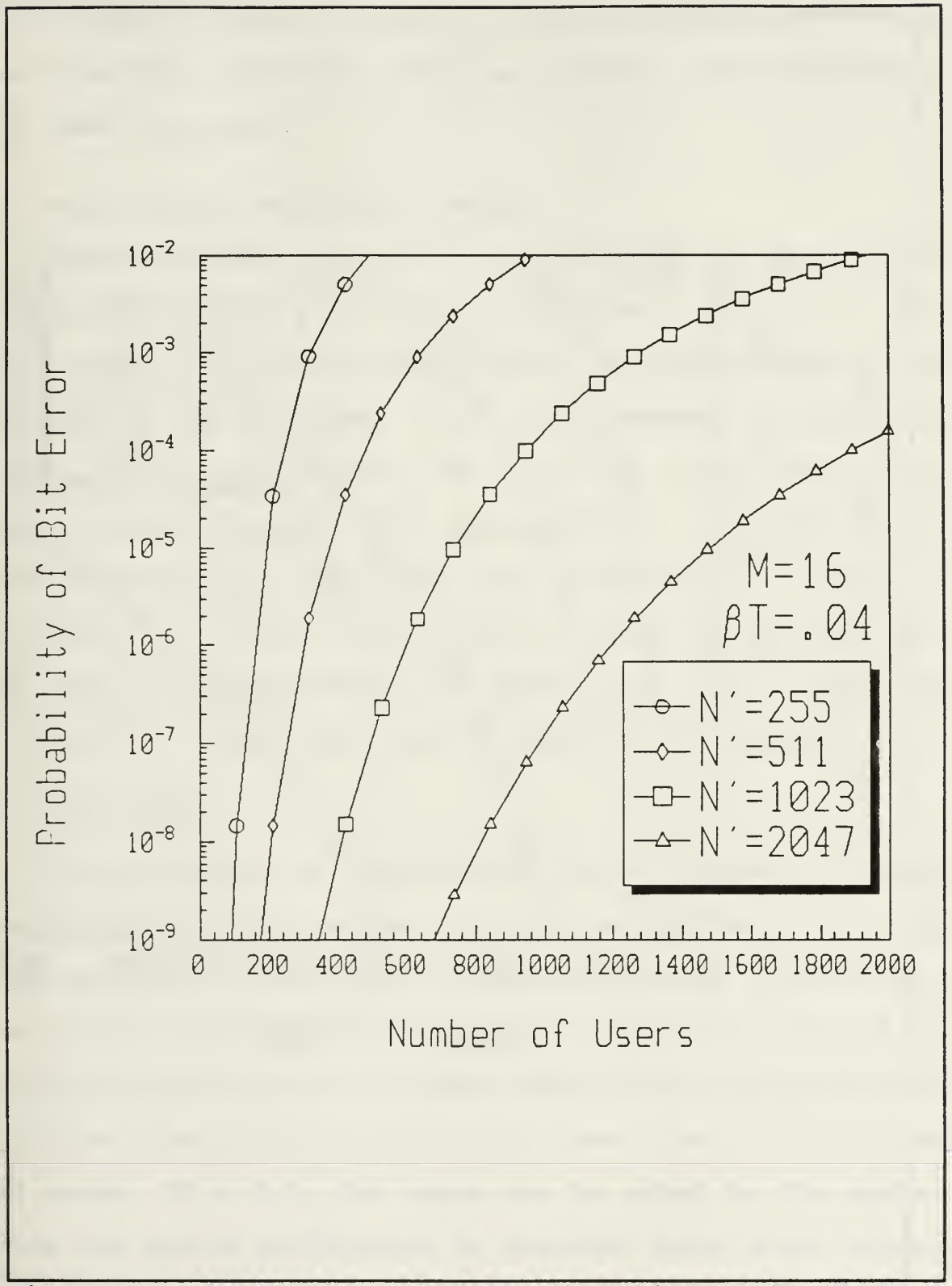

Figure 30 Performance of Coherent Optically Heterodyned MFSK-CDMA, M = 16 and βT = .04

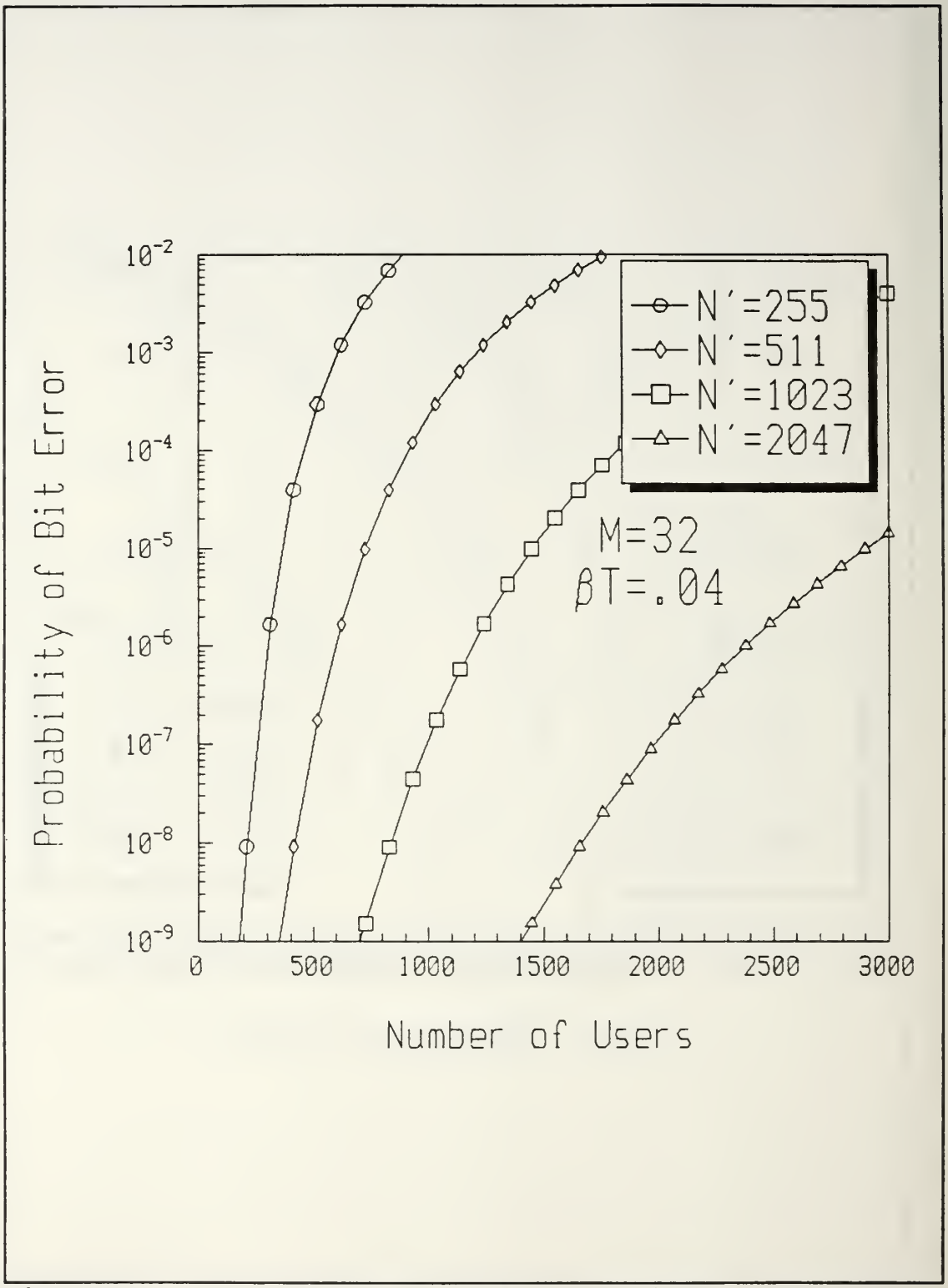

Figure 31 Performance of Coherent Optically Heterodyned MFSK-CDMA, M = 32 and βT = .04

five times the laser linewidth. This can be compared to 140 users for $\beta T = 0.01$ which requires a symbol rate of 100 times the laser linewidth.

C. Differential Phase-Shift Keying

The DPSK system analysis is performed by numerically evaluating Equation (93). This is plotted in Figure 32. The performance of the DPSK system shows the same trends as are observed in the MFSK case. The 3 dB improvement of DPSK over binary FSK is observed for the case when laser phase noise becomes negligible, $\beta T = 0.01$, as expected. Once again, a bit rate of twenty-five times the laser linewidth, $\beta T = 0.04$, is sufficient to overcome the effects of laser phase noise for the range of probability of bit error, 10^{-9} to 10^{-6}, that are of concern for practical digital communication systems.

D. DPSK-CDMA

The performance of the DPSK-CDMA system is found by using the noise term of Equation (99) in the probability of bit error expression, Equation (93), and numerically integrating. The results are plotted in Figure 33 for $\beta T = 0.1$ and in Figure 34 for $\beta T = 0.01$. The DPSK-CDMA results are consistent with that observed for the MFSK-CDMA case. For relatively low bit rates, $\beta T = 0.1$, few users can be added to the system since the system performance is degraded laser phase noise. For higher bit rates, $\beta T = 0.01$, then a larger number of users

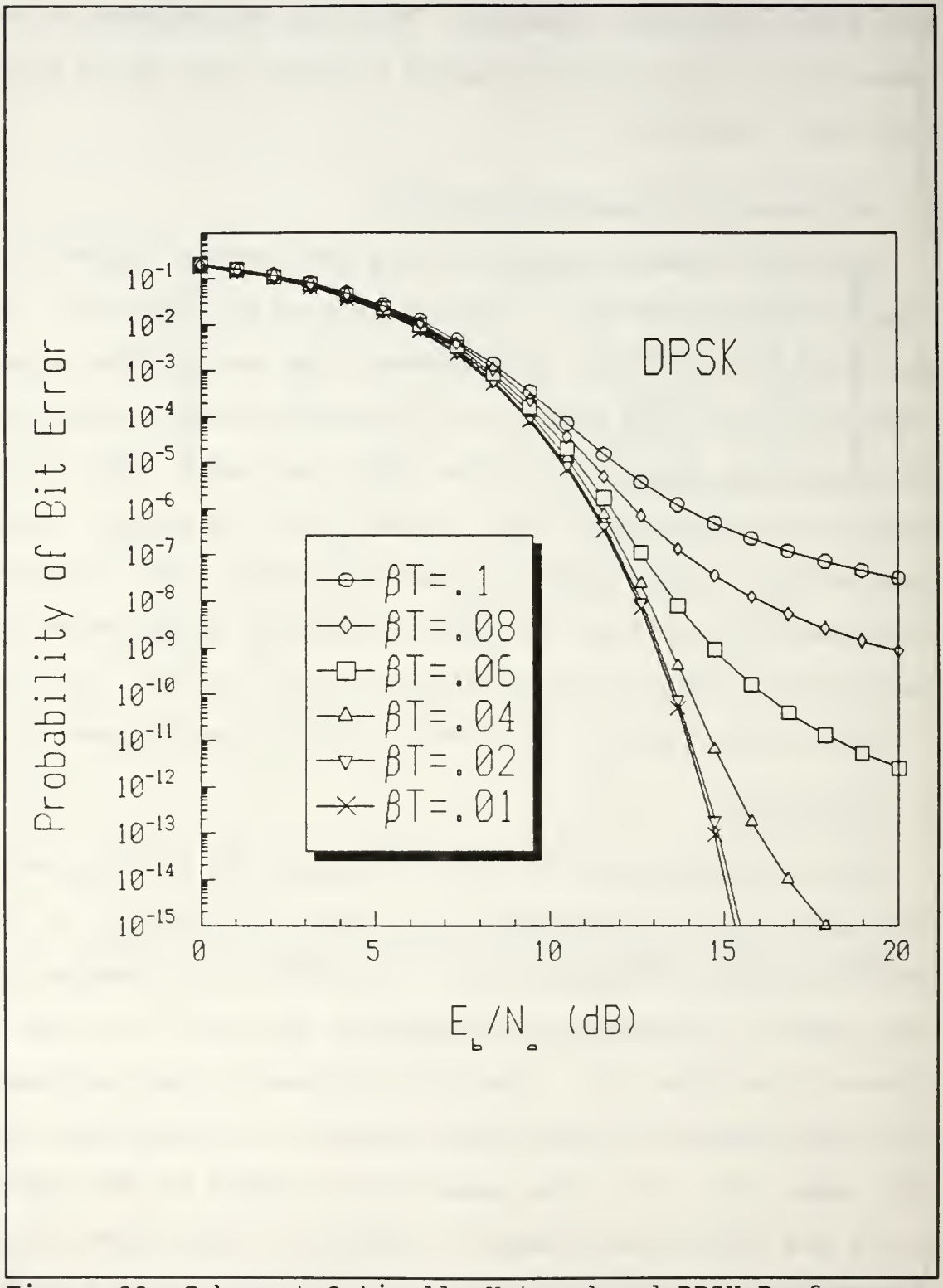

Figure 32 Coherent Optically Heterodyned DPSK Performance

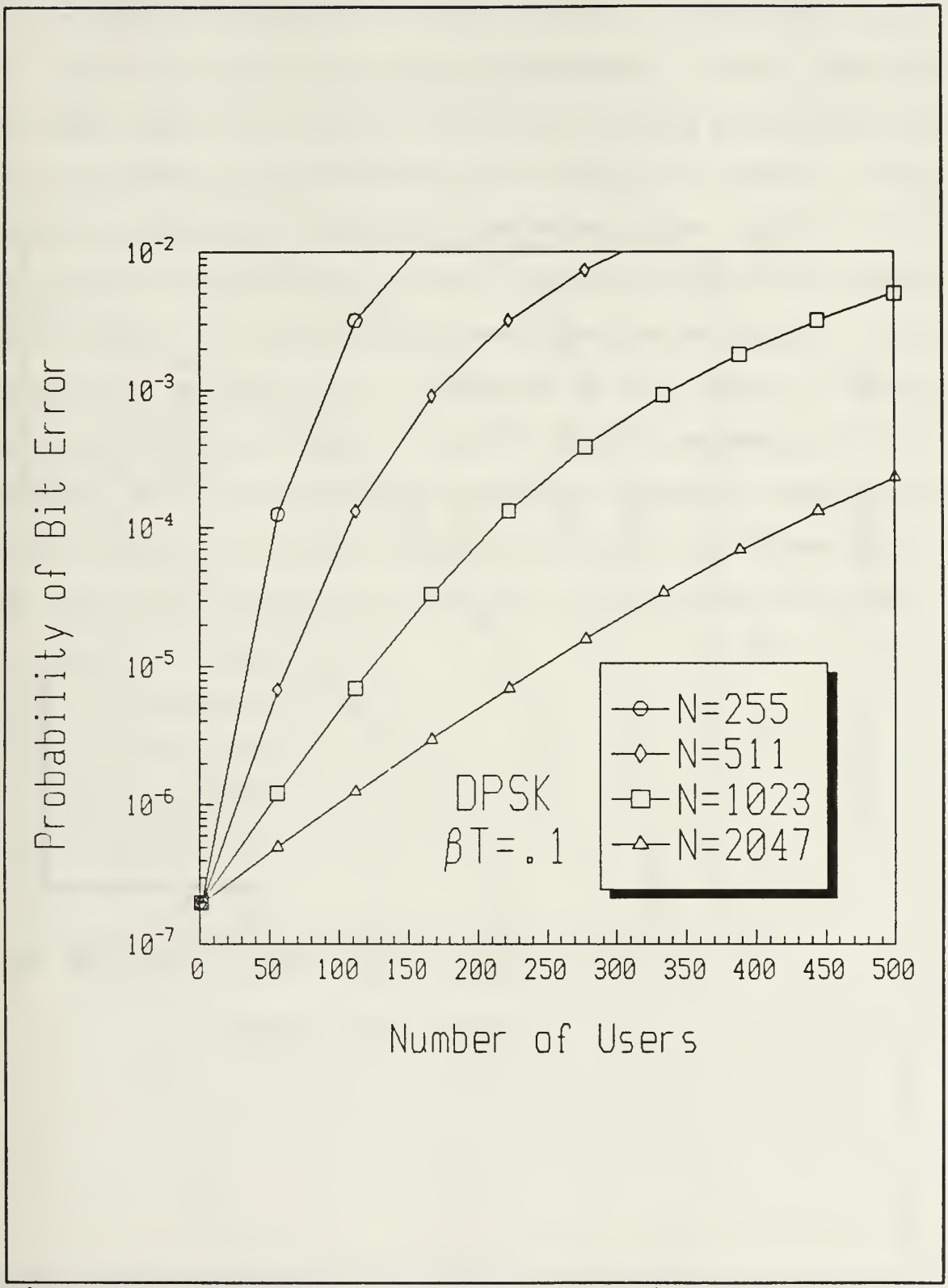

Figure 33 Performance of Coherent Optically Heterodyned DPSK, $\beta T = .1$

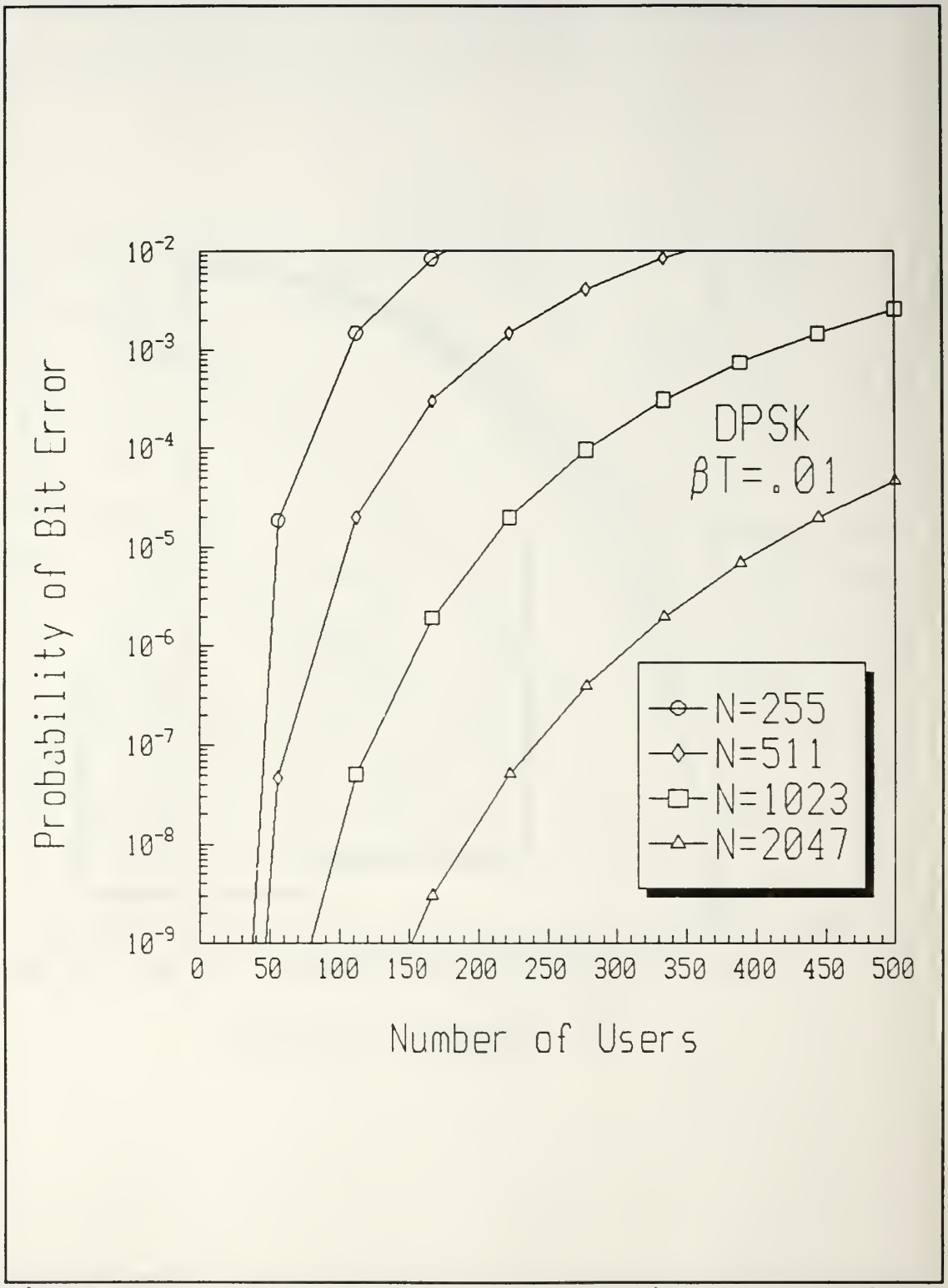

Figure 34 Performance of Coherent Optically Heterodyned DPSK, $\beta T = .01$

can be added to the system. The effect of laser phase noise no longer degrades the system performance. Just like the MFSK-CDMA case, for high bit rates the system performance is only affected by increasing the number of users. When observing the single user DPSK system analysis, for $\beta T = 0.04$ the system performance is only slightly affected by laser phase noise. The DPSK-CDMA system performance for $\beta T = 0.04$ is shown in Figure 35. An increase in the number of users from approximately 50 users for $\beta T = 0.1$ to approximately 140 users for $\beta T = 0.04$ is observed assuming a maximum probability of bit error of 10^{-6} and a codelength of 1023. Increasing the bit rate another factor of four, $\beta T = 0.01$, yields 150 users, an increase of only ten.

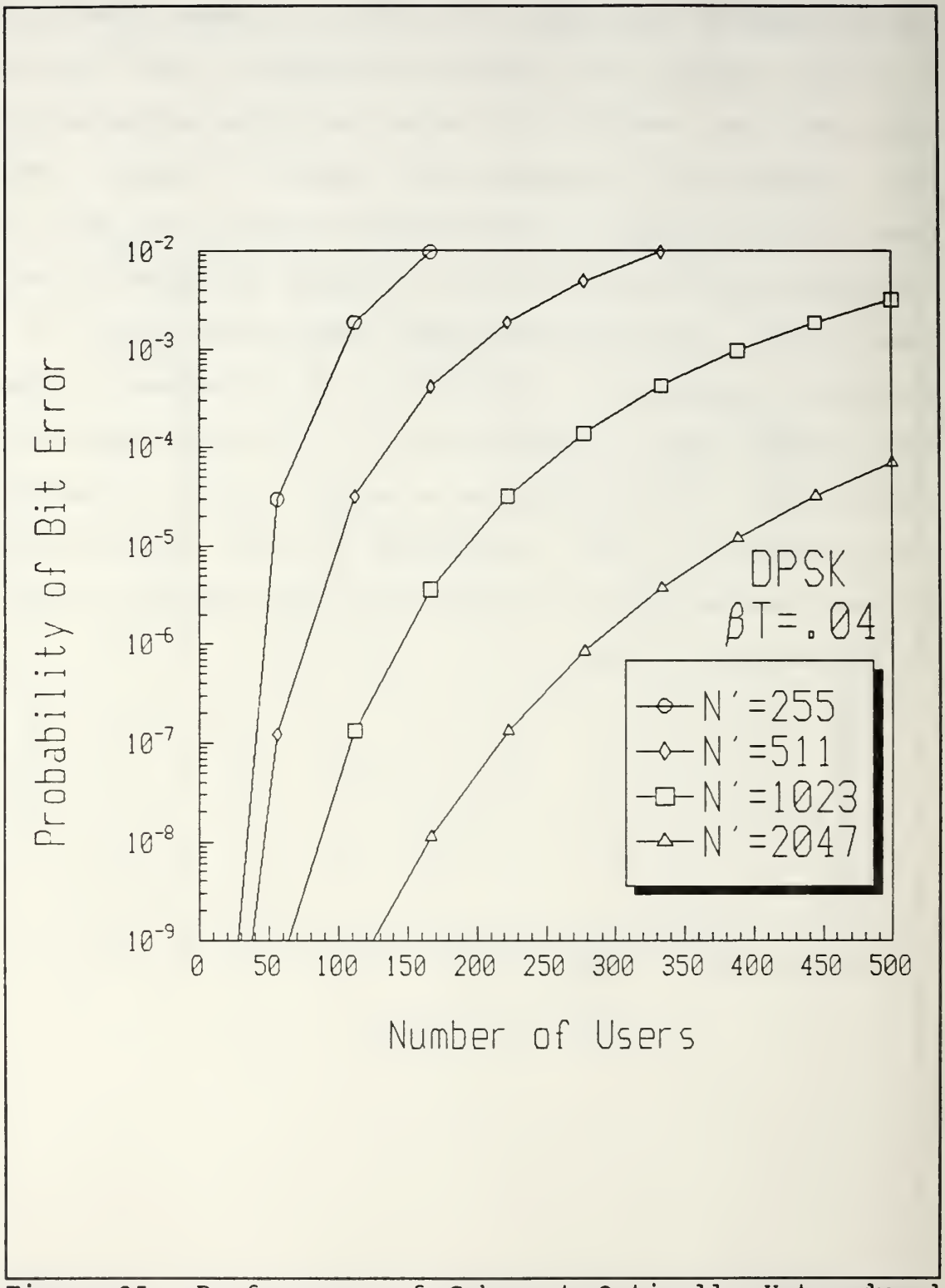

Figure 35 Performance of Coherent Optically Heterodyned DPSK, $\beta T = .04$

VI. CONCLUSIONS

This thesis investigates the system performance of two coherent optically heterodyned multiple access communication systems, MFSK-CDMA and DPSK-CDMA. The effect of laser phase noise that is inherent in coherent optical communication systems is analyzed for the single user communication system as well as the multiple user system. The analysis of the multiple access system helps to provide insight to the utility of MFSK-CDMA and DPSK-CDMA as possible random access, high data rate communication systems of the future.

The effect laser phase noise that exists in coherent optical communication systems can be minimized by increasing the data rate of the system. When the symbol rate for MFSK or the bit rate for DPSK is raised to a value of twenty-five times greater than the combined laser linewidth of the transmit and local oscillator lasers, system performance is only slightly affected by laser phase noise. This result holds for the probability of bit error values between 10^{-9} and 10^{-6}. System performance is virtually unaffected by laser phase noise when the data rate is increased to 100 times the laser linewidth.

The application of CDMA spread spectrum techniques to coherent optically heterodyned communication systems better utilizes the optical channel by allowing simultaneous

asynchronous access by multiple users. This thesis has shown that more users can be added to the multiple access system by increasing the codelength or by reducing the effects of laser phase noise by increasing the data rate. When the effect of laser phase noise is reduced then the number of users can be increased using a higher M for MFSK. All of these improvements occur at the expense of increasing the amount of bandwidth required. For an optical communication system, limiting the required bandwidth is not an overriding design consideration. As shown in Chapter V, a significant increase in the number of users can be achieved if the data rate is increased from ten times the laser linewidth to twenty-five times the laser linewidth. Only a minimal increase in the number of users will occur if the data rate is raised even higher.

Future research is needed in the areas of coherent optical communications and in the area of fiber optic CDMA communication systems. This work involved optical heterodyning and electronic demodulation of the received signal. Research is ongoing in the areas of optical demodulation [Ref. 1,3] and in the optical processing of CDMA systems [Ref. 13]. An all optical system will improve system performance due to the increased speed of optical processing and wider possible bandwidths.

This thesis performed theoretical analyses of the coherent optically heterodyned communication systems with MFSK-CDMA and

DPSK-CDMA signalling. Simplifying assumptions are made to ease the mathematical analysis. Some of the system requirements, such as maintaining polarity and coherently demodulating CDMA, are difficult to achieve which may affect system performance. The best evaluation of the performance of any system would be the actual construction and testing of the system. This thesis indicates that such a system configuration can improve the performance of future optical communication systems.

REFERENCES

1. Salz, J. "Coherent Lightwave Communications," AT&T Technical Journal, Vol. 64, No. 10, pp. 2153-2207, December 1985.

2. Vodhanel, R., "Optical Sources for Coherent Optical Fiber Communications," Proceedings of SPIE, Vol. 568, pp. 9-13, August 1985.

3. Okoshi, T. and Kikuchi, K., Coherent Optical Fiber Communications, Kluwer Academic Publishers, 1988.

4. Powers, J., "An Introduction to Fiber Optic Systems," Class Notes from EC 3550, Naval Postgraduate School, Monterey, CA, September 1990.

5. Brain, M. and Lee, T., "Optical Receivers for Lightwave Communication Systems," Journal of Lightwave Communications, Vol. LT-3, No. 6, pp. 1281-1300, December 1985.

6. Foschini, G., Greenstein, L. and Vannucci, G., "Envelope Statistics for Filtered Optical Signals Corrupted by Phase Noise," IEEE Transactions on Communications, Vol. 37,No. 12, December 1989.

7. Geraniotis, E., "Performance of Noncoherent Direct-Sequence Spread-Spectrum Multiple-Access Communications," Journal of Lightwave Technology, Vol. LT-3, No. 1, February 1985.

8. Whalen, A., Detection of Signals in Noise, Academic Press, 1971.

9. Foschini, G., Greenstein, L., Vannucci, G., "Noncoherent Detection of Coherent Lightwave Signals Corrupted by Laser Phase Noise," IEEE Transactions on Communications, Vol. 36, No. 3, pp. 306-314, March 1988.

10. Beyer, W., CRC Standard Mathematical Tables, CRC Press, Inc., 1981.

11. Sklar, B., Digital Communications, Prentice Hall, 1988.

12. Turin, G., "The Effects of Multipath and Fading on the Performance of Direct-Sequence CDMA Systems," IEEE Journal on

Selected Areas in Communications, Vol. SAC-2, No. 4, pp. 597-603, July 1984.

13. Prucnal, P., Santoro, M., Fan, T., "Spread Spectrum Fiber-Optic Network Using Optical Processing," Journal of Lightwave Technology, Vol. LT-4, No. 5, May 1986.

INITIAL DISTRIBUTION LIST

1.	Defense Technical Information Center Cameron Station Alexandria, VA 22304-6145	2
2.	Library, Code 52 Naval Postgraduate School Monterey, CA 93943-5000	2
3.	Chairman, Code EC Department of Electrical and Computer Engineering Naval Postgraduate School Monterey, CA 93943-5000	1
4.	Professor R. C. Robertson, Code EC/Rc Department of Electrical and Computer Engineering Naval Postgraduate School Monterey, CA 93943-5000	5
5.	Professor T. T. Ha, Code EC/Ha Department of Electrical and Computer Engineering Naval Postgraduate School Monterey, CA 93943-5000	1
6.	LT David A. Jakubek, USN Code 80, SOAC Class 92030 Box 700 Groton, CT 06349-7000	2
7.	LT Kent Varnum Naval Ordinance Missile Test Station White Sands Missile Range, NM 88002	1

Thesis
J245 Jakubek
c.1 Coherent/noncoherent detection of coherent optical heterodyne DPSK-CDMA and MFSK-CDMA signals.